



2014

## CONVERGENCE OF DUNE TOPOGRAPHY AMONG MULTIPLE BARRIER ISLAND MORPHOLOGIES

Jackie Ann Monge

University of Kentucky, [jackie.monge@uky.edu](mailto:jackie.monge@uky.edu)

[Right click to open a feedback form in a new tab to let us know how this document benefits you.](#)

---

### Recommended Citation

Monge, Jackie Ann, "CONVERGENCE OF DUNE TOPOGRAPHY AMONG MULTIPLE BARRIER ISLAND MORPHOLOGIES" (2014). *Theses and Dissertations--Geography*. 19.  
[https://uknowledge.uky.edu/geography\\_etds/19](https://uknowledge.uky.edu/geography_etds/19)

This Master's Thesis is brought to you for free and open access by the Geography at UKnowledge. It has been accepted for inclusion in Theses and Dissertations--Geography by an authorized administrator of UKnowledge. For more information, please contact [UKnowledge@lsv.uky.edu](mailto:UKnowledge@lsv.uky.edu).

## **STUDENT AGREEMENT:**

I represent that my thesis or dissertation and abstract are my original work. Proper attribution has been given to all outside sources. I understand that I am solely responsible for obtaining any needed copyright permissions. I have obtained needed written permission statement(s) from the owner(s) of each third-party copyrighted matter to be included in my work, allowing electronic distribution (if such use is not permitted by the fair use doctrine) which will be submitted to UKnowledge as Additional File.

I hereby grant to The University of Kentucky and its agents the irrevocable, non-exclusive, and royalty-free license to archive and make accessible my work in whole or in part in all forms of media, now or hereafter known. I agree that the document mentioned above may be made available immediately for worldwide access unless an embargo applies.

I retain all other ownership rights to the copyright of my work. I also retain the right to use in future works (such as articles or books) all or part of my work. I understand that I am free to register the copyright to my work.

## **REVIEW, APPROVAL AND ACCEPTANCE**

The document mentioned above has been reviewed and accepted by the student's advisor, on behalf of the advisory committee, and by the Director of Graduate Studies (DGS), on behalf of the program; we verify that this is the final, approved version of the student's thesis including all changes required by the advisory committee. The undersigned agree to abide by the statements above.

Jackie Ann Monge, Student

Dr. Jon Anthony Stallins, Major Professor

Dr. Patricia Ehrkamp, Director of Graduate Studies

CONVERGENCE OF DUNE TOPOGRAPHY  
AMONG MULTIPLE BARRIER ISLAND MORPHOLOGIES

---

THESIS

---

A thesis submitted in partial fulfillment of the requirements for the degree of Master of  
Arts in the College of Arts and Sciences at the University of Kentucky

By

Jackie Ann Monge

Lexington, Kentucky

Co-Directors: Dr. Jon Anthony Stallins, Associate Professor of Geography  
and Dr. Daehyun Kim, Associate Professor of Geography

Lexington, Kentucky

2014

Copyright © Jackie Ann Monge 2014

## ABSTRACT OF THESIS

### CONVERGE OF DUNE TOPOGRAPHY AMONG MULTIPLE BARRIER ISLAND MORPHOLOGIES

Wave-dominated and mixed tidal and wave energy barrier islands are assumed to have characteristic dune topographies that link to their macroscale form. However, there has been no systematic attempt to describe the linkage between barrier island macroscale form and dune topography. The goal of this thesis was to investigate how dune topographies correspond to a number of barrier island morphologies found along the southeastern U.S. Atlantic coast. Macroscale process-form variables were used to classify 77 islands into seven morphologic clusters. Islands from each cluster were selected and sites characteristic of the range of dune topographies within islands were characterized using three methods: the frequency distribution of elevations, directional spatial autocorrelation of elevation at different distance classes, and FRAGSTATS indices summarizing the patch structure of elevations. Variables derived from each of these methods peaked in their ability to discriminate among barrier island morphologies when the islands were aggregated into three groups. An ordination of those variables revealed a two or three-fold grouping of barrier island dune types that approximated the traditional wave dominated and mixed energy barrier island morphologic classification. These findings suggest that dune topographies converge upon two to three configurations even within the heterogeneity in macroscale island morphology.

**KEYWORDS:** Barrier island morphology, Dune topography, Coastal classification, Multivariate analysis, Thresholds

Jackie Ann Monge  
May 7, 2014

CONVERGENCE OF DUNE TOPOGRAPHY  
AMONG MULTIPLE BARRIER ISLAND MORPHOLOGIES

By

Jackie Ann Monge

Dr. Jon Anthony Stallins  
Co-Director of Thesis

Dr. Daehyun Kim  
Co-Director of Thesis

Dr. Patricia Ehrkamp  
Director of Graduate Studies

May 7, 2014

## ACKNOWLEDGEMENTS

I thank Dr. Tony Stallins and Dr. Daehyun Kim, my advisors, and Dr. Jonathan Phillips for teaching me how to be a better earth scientist. Your insights and tutelage helped me grow as a scholar and reminded me of the value of my work. I look forward to your continuing mentorship and friendship throughout my career.

I want to extend my gratitude to those professors and students involved in the Biogeomorphology Reading and Analysis Group and the Political Ecology Working Group for thought provoking discussions, feedback, and fun times. Thank you to Lori Tyndall, my graduate student colleagues, and especially my cohort: Andrew A., Jay B., Andrea C., Brittany C., Dan C., Anna G., Kayla H., Marita M., Megan W., Lindsay S., Sophie S., and Sara S. for your encouragement and perspective. I would also like to thank Dr. Elise Gornish for her advice and friendship through the years.

I appreciate and am thankful for Dr. Kelly W., Sophie W., Kate S., Sara S., Pete D., Tara M., Matt M., Pierce M., and Dr. Lynn P. for making me feel comfortable and at home in Kentucky.

I am eternally grateful for Yasmin and Maximo, my mother and father, who have sacrificed so much for my benefit. They have always emphasized the importance of education which has been the prime reason for my professional success. Thank you to Michelle, Mark, Shadow (our puppy), and my extended family for believing in me.

Last and certainly not least, I would like to thank Michael for encouraging my dreams, enduring stressful times, and his unconditional support.

## TABLE OF CONTENTS

|   |     |
|---|-----|
| Acknowledgements .....  | iii |
| List of Tables .....  | v   |
| List of Figures .....   | vi  |
| Chapter One: Introduction .....   | 1   |
| Chapter Two: Background .....   | 5   |
| Chapter Three: Methods .....  | 13  |
| Study area .....  | 13  |
| Research question 1 .....   | 13  |
| Barrier island classification data .....  | 13  |
| Barrier island morphology classification .....  | 14  |
| Research question 2 .....   | 14  |
| Dune topography sampling and LIDAR mapping .....  | 15  |
| Area of interest (AOI) sites .....  | 15  |
| Resampling and interpolation .....  | 16  |
| Characterizing dune topography .....  | 16  |
| Descriptive statistics .....  | 17  |
| Correlograms .....  | 17  |
| Landscape indices .....   | 17  |
| Comparing dune topographies .....   | 19  |
| Chapter Four: Results .....   | 22  |
| Barrier island macroscale morphology .....  | 22  |
| Dune topographies .....   | 23  |
| Dune metrics for individual island sites .....  | 24  |
| PCoA of dune metrics .....  | 25  |
| Chapter Five: Discussion .....  | 52  |
| Overview .....  | 52  |
| Chapter Six: Conclusions .....  | 55  |
| Appendices .....  | 58  |
| Appendix A: Islands studied and the variables used to classify their<br>macroscale morphology ..... | 58  |
| Appendix B: Descriptive variables derived from elevation data corresponding<br>to each AOI .....    | 60  |
| Appendix C: FRAGSTATS variables derived from reclassified rasters for<br>each AOI .....             | 61  |
| References .....  | 62  |
| Vita .....  | 68  |

## LIST OF TABLES

|   |    |
|---|----|
| Table 3.1, Description of island sites sampled .....  | 20 |
| Table 4.1, Indicator Values (IV) and associated p-values for 5, 6, and 7 macroscale groupings derived from Indicator Species Analysis on macroscale variables .....             | 28 |
| Table 4.2, Spearman's correlation analysis between original island macroscale variable and PCoA axis scores .....   | 29 |
| Table 4.3, Macroscale island cluster summary .....  | 30 |
| Table 4.4, Islands for each of the clusters as derived from PCoA and hierarchical and agglomerative clustering .....  | 31 |
| Table 4.4, Islands for each of the clusters as derived from PCoA and hierarchical and agglomerative clustering .....  | 31 |
| Table 4.5, Indicator Values (IV) and associated p-values for 2, 3, 4, 5, and 6 macroscale groupings derived from Indicator Species Analysis on dune topographic variables ..... | 32 |



## LIST OF FIGURES

|  |    |
|--|----|
| Figure 2.1, Hayes' microtidal (left) and mesotidal (right) barrier island morphologies.....  | 10 |
| Figure 2.2, Leatherman's (1978) coarse continuum classification of barrier island morphologies .....   | 11 |
| Figure 2.3, Williams and Leatherman's (1993) barrier island morphologies .....   | 12 |
| Figure 3.1, Study area .....   | 21 |
| Figure 4.1, Cluster dendrogram of major barrier island morphologic groups.<br>Dashed lines indicate hierarchical divisions into 2, 3, 4, 5, 6, and 7 barrier island groupings.....   | 33 |
| Figure 4.2, PCoA ordination of barrier island macroscale variables .....   | 34 |
| Figure 4.3, Distribution of island clusters along the coastline .....  | 35 |
| Figure 4.4a, Parramore Island, Cluster 2, and AOIs (in red) .....  | 36 |
| Figure 4.4b, South Core Banks, Cluster 3, and AOIs (in red).....   | 37 |
| Figure 4.4c, Bull Island, Cluster 4, and AOIs (in red) .....   | 38 |
| Figure 4.4d, Kiawah Island, Cluster 5, and AOIs (in red) .....   | 39 |
| Figure 4.4e, Sapelo Island, Cluster 6, and AOIs (in red).....  | 40 |
| Figure 4.4f, Cape Canaveral, Cluster 7, and AOIs (in red).....   | 41 |
| Figure 4.5, Frequency distribution of elevations among AOIs for each island sampled.<br>The solid black line is the 50th percentile (median) elevation. The top and bottom of the box plot indicate the 75th and 25th percentile respectively.<br>Points outside of the whiskers indicate outlier elevations ..... | 42 |
| Figure 4.6, Correlograms produced for AOIs A (northernmost) thru B (southernmost) on each representative island. Distance classes (in meters) are plotted on the x-axis and Moran's I values, which range from 0 (negative autocorrelation) to 1 (positive autocorrelation), are plotted on the y-axis .....       | 43 |
| Figure 4.7, Reclassified AOIs A (northernmost) thru B (southernmost) used for deriving FRAGSTATS indices. AOIs differed in their dimensions. Values on the bottom right of each AOI indicate their true size relative to the largest AOI, South Core Banks C ( $X = 215 \text{ m}^2$ ) .....                       | 44 |
| Figure 4.8, PCoA of spatial autocorrelation data.....  | 45 |
| Figure 4.9, PCoA of dune variables AI, PAFRAC, SHAPE_AM and Mean.....  | 46 |
| Figure 4.10a, PCoA plot for AI. On bottom left corner of the scatterplot are correlation coefficients r (Pearson) and tau (Kendall) for axis scores and variables. Size of each correlation coefficient reflects the magnitude of the variable.....  | 47 |
| Figure 4.10b, PCoA plot for PAFRAC.....  | 48 |
| Figure 4.11a, PCoA plot for SHAPE_AM.....  | 49 |
| Figure 4.11b, PCoA plot for mean elevation. ....   | 50 |
| Figure 4.12, PCoA of dune topographic state space.....   | 51 |

## CHAPTER ONE: INTRODUCTION

Large stretches of sandy coastline have been classified in terms of physical or biological properties, modes of evolution, or geographic occurrence (Davies, 1964; Finkl, 2004). They have also been classified in terms of wave, wind, and tidal energy gradients (Hayes, 1979; Davis, 1994). In other cases, classifications have relied upon local descriptors such as coastline configuration (Bartley et al., 2001), and the extent of foredune habitats and plant species (Doing, 1985). Sandy coasts have also been categorized according to morphological response type and potential response to rising sea levels (McBride et al., 1995; Hapke et al 2013).

Categorization and classification of the shoreline is necessary to address the complexity of factors impinging upon coastal zones. These include the anticipated effects of global climate change within the next century (Feagin et al., 2005; Jackson et al., 2013). With rising sea-levels (FitzGerald et al., 2008; Engelhart et al., 2009), the uncertainties surrounding the likelihood for greater extratropical and tropical storm activity (Coumou and Rahmstorf, 2012; Grinsted et al., 2012; Woodruff et al., 2013), and vulnerable populations and property along the coast (Strauss et al., 2012; Arkema et al., 2013) a central question remains as to how stretches of coastline might be expected to vary in their responses to more frequent high water events.

For this study, I examined the relationship between dune topography and barrier island morphology. Barrier islands are coastal landforms that serve to protect mainland areas from the full effects of tropical and extratropical storms (Zhang and Leatherman, 2011; Otvos, 2012; Temmerman et al., 2013; Arkema et al., 2013; Spalding et al., 2013). While many members of the public have ignored the structural benefits of these structures (Schlacher et al., 2008; Everard et al., 2010), their presence is critical to the stability of coastal areas along the southeastern U.S. where they protect mainland areas from significant offshore wave action. Iconic of these islands are their dune features. As many coastal scholars have emphasized, understanding how to maintain the mobility of dunes in varied contexts might ensure the persistence of overall barrier functions (Feagin et al., 2010).

This thesis investigated how barrier island morphologies correspond to their underlying

dune topographies. Specifically, to what extent do broad scale process-based barrier island morphologies exhibit propensities to develop similar dune topographies? Longstanding classifications of barrier islands make a distinction between two general types of barrier island morphology (microtidal and mesotidal) and posit that each has distinctive dune topographies. Yet given the readily visible heterogeneity that exists in barrier island form, how generalizable is this assumption? Do distinctive types of dune topographies correspond to particular groupings of barrier island morphology? While it is a truism to state that the dunes of any island are different from all others, this assumption does not consider the degree to which an island may be comprised of variable topographies, some of which may more closely resemble topographies of other islands. The methods developed for this study aimed to determine the grouping of barrier island morphologies that maximizes between-island differences in underlying topography types, while minimizing topographic contrasts within these islands.

Coastal research in general is recognized for its division between individual-island process studies or broad scale evolutionary or descriptive classifications. Many of the original studies of coastal barrier landforms invoked classifications based on processes occurring over broad areas (Hayes, 1979). However, over the intervening decades there have been a large number of individual-island based studies. Process-based field studies often take measurements over small temporal and spatial scales, and by necessity, often become restricted to single island locations. Recently, these two spatial scales of reference have been undergoing integration. The Coastal Vulnerability Index combined broad scale factors, such as wave and tidal energy, with local variations in land elevation to determine both erosion and inundation risk along the U.S. coastline (Gornitz, 1991). DHigh is an example of a similar integration. It incorporates factors such as wave influence and frontal dune height to forecast along-shore variability due to long and short-term processes of coastal erosion (Elko et al., 2002). These approaches cover a wide area and integrate local detail. However, they do not aim to integrate scales or examine the geographic patterning arising from cross-scale relationships.

Drawing linkages between broad-scale pattern and its local particularities is a fundamental challenge of geography. Human geographers have sought to link scales such as the global and the local through what was known as the localities debate. Physical geographers have sought to undo broad continuum approaches by

emphasizing the relevance of local controls. Coastlines have had far less formal scrutiny in this regard, excepting the literature regarding the fractal nature of coastlines in general (see Phillips, 1986). In this study, I investigated how macroscale barrier island morphology links to local dune topography. The study area encompassed the southeastern U.S. Atlantic coastline, the setting for the development of some of the first classifications of barrier island morphology and the descriptions of their characteristic topography. These classifications are based on continuum concepts which hold that broad gradients in wave energy and tidal range give rise to broad trends in barrier island macroscale morphology. On mixed wave and tidal energy coastal areas one can find mesotidal barrier islands, which exhibit prominent ridge and swale dune topography that redirects storm surge and overwash to tidal inlets. Alternatively, in wave-dominated regions one can find microtidal barrier islands. These islands are generalized as having low topography and respond to high water events through direct overwash and retreat.

For coastal management, there is a need to understand how consistent these macroscale-microscale linkages are. To what extent can island morphologies provide an inference about local dune topography? Formally, the goal of this study was to examine categorizations of island morphology and the generalizations about their underlying dune topographies. I investigated the following two questions: 1) *What are the distinctive groupings of macroscale barrier island morphology?* and 2) *How do dune topographic types correspond to these groupings of barrier island morphology?* To address the first question, I undertook a multivariate classification of barrier island morphologies. It built upon the study by Williams and Leatherman (1993), who performed a classification of barrier island morphologies long before the ease of access to geographic information systems (GIS) software, open data, and Google Earth. I repeated their study using GIS and more advanced computational procedures. For the second question, it was first necessary to develop methods to characterize dune topographies for each of the island clusters determined in my first question. I then assessed how well the variables obtained from each of these methods discriminated among different hierarchical clusters of barrier island morphologies. In this manner, it was possible to parsimoniously characterize dune topographic types and how well they mapped onto different groupings of barrier island morphologies. The motivation for this thesis was to understand how relationships among barrier island morphology and dune topography relate to one another geographically,

which may in turn be useful for conceptualizing responses to high water events over larger areas and among a number of islands (Masselink and van Heteren, in press).

## CHAPTER TWO: BACKGROUND

How barrier islands along the coastal plain of the U.S. might respond to high water events has been a subject of inquiry in the scientific community for several decades. Much of our current understanding of how barrier islands might respond to rising sea level goes back to the pioneering coastal research that led to classifications for barrier island morphology (Hayes, 1979; Davis and Hayes, 1984). Hayes (1979) summarized barrier island morphology as the function of two main macroscale morphometric variables: tidal range and wave height. Under wave-dominated conditions, which most commonly occur in microtidal areas (tidal range  $\leq 2$  m), the barriers are long, typically tens of kilometers, with widely spaced inlets that have large flood-tidal deltas and small ebb-tidal deltas. Toward the landward side of these islands one can typically find bays and/or lagoons. Barrier islands along mixed-energy coasts, which typically occur in mesotidal areas (tidal range 2–4 m), are stunted and short (usually  $< 10$  km) with abundant tidal inlets that contain large ebb-tidal deltas and small to nonexistent flood-tidal deltas. These islands are flanked on the landward side by complex tidal channels, tidal flats, and wetlands.

In recognition of the morphodynamics embedded in these classifications, part of the classification of these barrier islands include how they respond to high water events. The ridge and swale topography on the classic “drumstick” shaped mesotidal barrier islands (**Figure 2.1**) deflect storm surge and overwash toward numerous tidal inlets leading inland and into dense networks of tidal salt marsh creeks. Microtidal barrier islands (**Figure 2.1**) have low topographic profiles that permit overwash to penetrate inland. Following Hayes’ work, broad continuum approaches conceptualized the coast into stretches of island morphologies. Leatherman (1978) mapped these morphologies along the U.S. Atlantic coast (**Figure 2.2**), and subsumed in these classifications are their expected responses to high water events. Microtidal coasts are more likely to experience overwash, while mesotidal barrier coasts are not, and when it does occur it will be of a fundamentally different character.

Bights, such as the Georgia Bight, approximate broad gradients at course scales. However, the classic continuum approach to barrier island morphology has been recognized as not entirely valid. Barrier landforms are now recognized as occurring in a

wider range of contexts, allowing for a greater range of forms and processes than expressed in earlier continuum approaches (Stutz and Pilkey, 2002; Stutz and Pilkey, 2011). Shoreline configuration can reflect historical processes as well as ongoing modification by near-shore dynamics (Murray et al., 2001). Moreover, it is the relative contrast in wave energy and tidal range that shapes barrier island morphology (Davis and Hayes 1984). Recognizing that these continuum concepts are more heterogeneous, Williams and Leatherman (1993) used both form and process macroscale variables to classify barrier islands along the U.S. Atlantic coast into five groups, each of which corresponded to a particular morphologic type (**Figure 2.3**). Class A islands were distinguished by their extended width and corresponded with the mesotidal barrier islands of Hayes' classification (e.g. tide-dominated mixed-energy). Class B islands were delineated by their narrow width. Class C islands were grouped on the basis of their extended length and corresponded to the microtidal barrier island types described by Hayes (e.g. wave dominated mixed-energy islands). Alternatively, Class D islands were grouped based on their short length. Finally, Class E consisted of islands grouped in terms of their orientation relative to the shoreline.

Within individual islands, scholars have also expounded upon how local processes shape dune topography and potential responses to high water events that are not necessarily linked to broader island morphology. Local processes are given precedence as to understanding the potential responses to high water events. Topography and its alongshore variation is a key factor in determining the local patterns of overwash and how coastal barriers flood (Hayden et al., 1995; Morton and Sallenger, 2003; Houser, 2013). The history and sequence of coastal storm landfalls (Houser and Hamilton, 2009; Houser et al., 2008) beach-dune sediment budgets (Psuty, 1988; Sherman and Bauer, 1993; Anthony, 2013; Davis, 2013), beach morphology and alongshore variability in dune topography (Hayden et al., 1995; Houser, 2013) geological history and antecedent topography (Evans et al., 1985; Riggs et al., 1995; Jackson et al., 2013), and temporal variability in wave regime (Anthony and Orford, 2002) may also factor into barrier dune topographic responses to high water events.

Thus barrier island morphology and local dune topography are two explanatory frameworks that make assumptions about how barrier coasts might respond to high water events. One attempts to make broader generalizations. The other takes local

detail into account but does not seek to generalize. For management officials who have to speak about potential responses to high water events along barrier coasts, referencing one of two barrier island morphologies alone may be too simplistic. Similarly, referencing the geomorphic idiosyncrasies of each barrier island can hinder articulation of how coastal zones over wider areas might respond to rising sea levels. If resilient coasts are to be designed using soft ecosystem approaches, a better understanding of the relationships between the scales of barrier island morphologies and dunes needs to be established.

The conceptual motivation of this thesis was to take a more geographic perspective on how macroscale barrier island morphology and local dune topography correspond and create a much more heterogeneous distribution of potential coastal behaviors to high water events. By classifying barrier island morphologies into similar clusters, and quantifying how dune topography varies between and within these barrier island groupings, I was able to assess the level at which one can generalize about barrier coasts and how they might respond to high water events. No two islands would be identical in their response to high water, a geographic observation of limited usefulness. However, the question is how similar island dune topographies are within the constraints of the larger macroscale barrier island process-form morphologies, and how their correspondence is distributed along the U.S. Atlantic coast. In this sense, my thesis contributes to discussions about the potential range of impacts in coastal zones as a result of forcings acting on an inhomogenous template of coastal conditions.

In the first part of my study, I performed a multivariate classification of barrier island morphologies. Computational power has increased considerably since Williams and Leatherman (1993) performed their classification of barrier island morphologies along the U.S. Atlantic coast. The use of non-parametric Monte Carlo-based methods of ordination and cluster detection permit more detailed assessments of island differences and similarities. These can now be more readily portrayed visually in statistical maps as well as in standard quantitative description. In the second part of my study, I characterized dune topography for representative islands in each of the macroscale clusters resulting from the aforementioned procedure. I accomplished this by calculating the frequency distribution of elevations, measuring spatial autocorrelation over various



distance classes, and computing FRAGSTATS indices from LIDAR topographic data for distinctive dune sites across islands.

There are conceptual analogs for this thesis. In physical geography, the River Continuum Concept describes how fluvial form and function parallel systematic upstream-downstream changes in discharge. However, this paradigm has been challenged by fluvial geomorphologists who have addressed more of the spatial complexity of rivers (Poole, 2002; Burchsted et al., 2010; Cushing et al., 2006; Thorp et al., 2010). In this thesis, I attempted to draw out more detail about the topographic heterogeneity in macroscale barrier island morphologic types organized along broad geographic continuums. It should be emphasized that I did not attempt to develop a taxonomic classification, a dichotomous key for the delineation of barrier island types and their expected topographic response to high water levels. What was intended was an assessment of how widely or how narrowly one can associate dune forms and processes to barrier island morphology. In this manner, my work addressed one of the fundamental goals of geography: the identification of fallacies of spatial thinking. In the individualistic fallacy, extrapolations are taken to the broad scale based on observations conducted at small, local scales. Assessment of barrier island topography on one island and making a generalization to other islands and how they might respond to rising sea levels invokes the individualistic fallacy. In the ecological fallacy, one makes local-scale characterizations based on broad-scale observations. In this situation, claims as to how an island might respond to rising sea levels are drawn from knowledge of how particular classes of islands are expected to respond. My study aimed to assess the extent at which these often necessary extrapolations and interpolations are robust.

In this study I retained the usage of the term *barrier island*, when it may be more broadly accurate to consider them as *barrier-related landforms* since some may be spits or barrier beaches (Leatherman, 1978). As Finkl (2004) recognized, classifications boil down to the definitions and nomenclature used. Indeed, the nomenclature and criteria for identifying barrier islands is complex and not entirely free of debate (Otvos, 2010). I referred to them as barrier islands given their capacity to absorb energy from storms and their potential to be where the processes of sea level rise are prominently visible, although there are a range of barrier landforms. In addition, I did not discriminate between the mode of origin of dunes on these structures, as is sometimes debated in

the difference over dune ridges and foredunes (Hesp, 2011). Dunes in this study have more of a functional identity given their ability to buffer rising sea levels and minimize exposure to hazards (Arkema et al., 2013). Implicit in this is that dune topography is a proxy for the sum of intersecting meteorological, geologic, ecological, and historical contingencies that influence dune development (Houser, 2009).

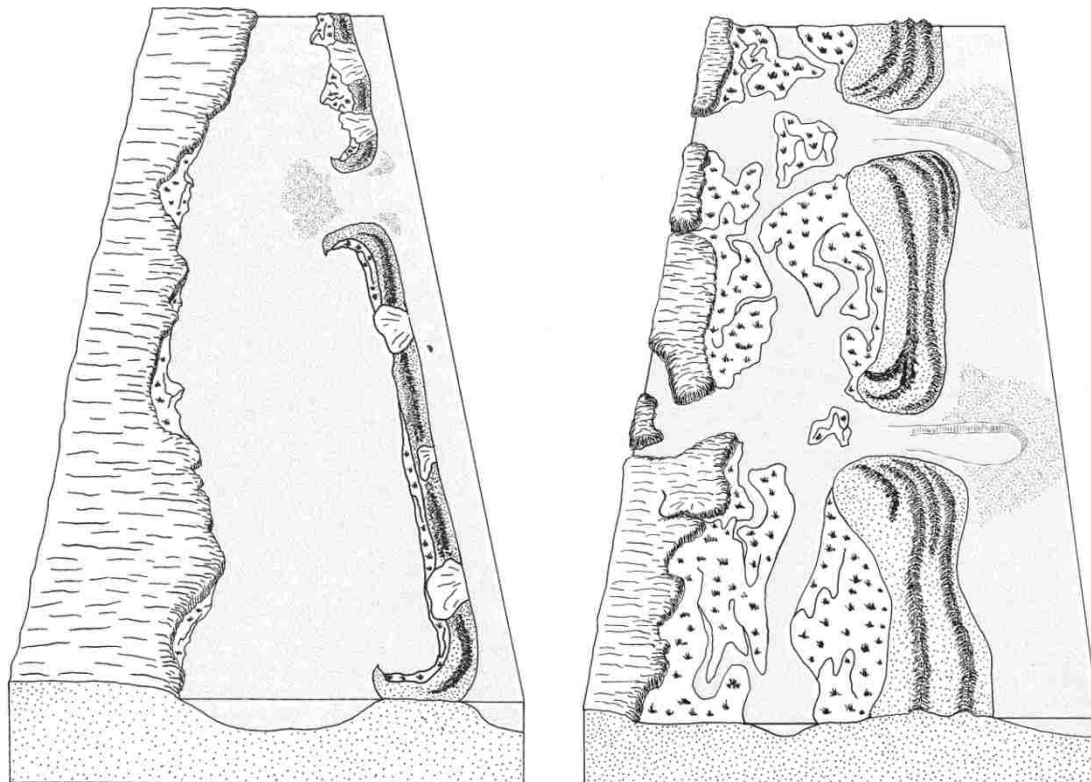


**Figure 2.1.** Hayes' microtidal (left) and mesotidal (right) barrier island morphologies.



**Figure 2.2.** Leatherman's (1978) coarse continuum classification of barrier island morphologies.

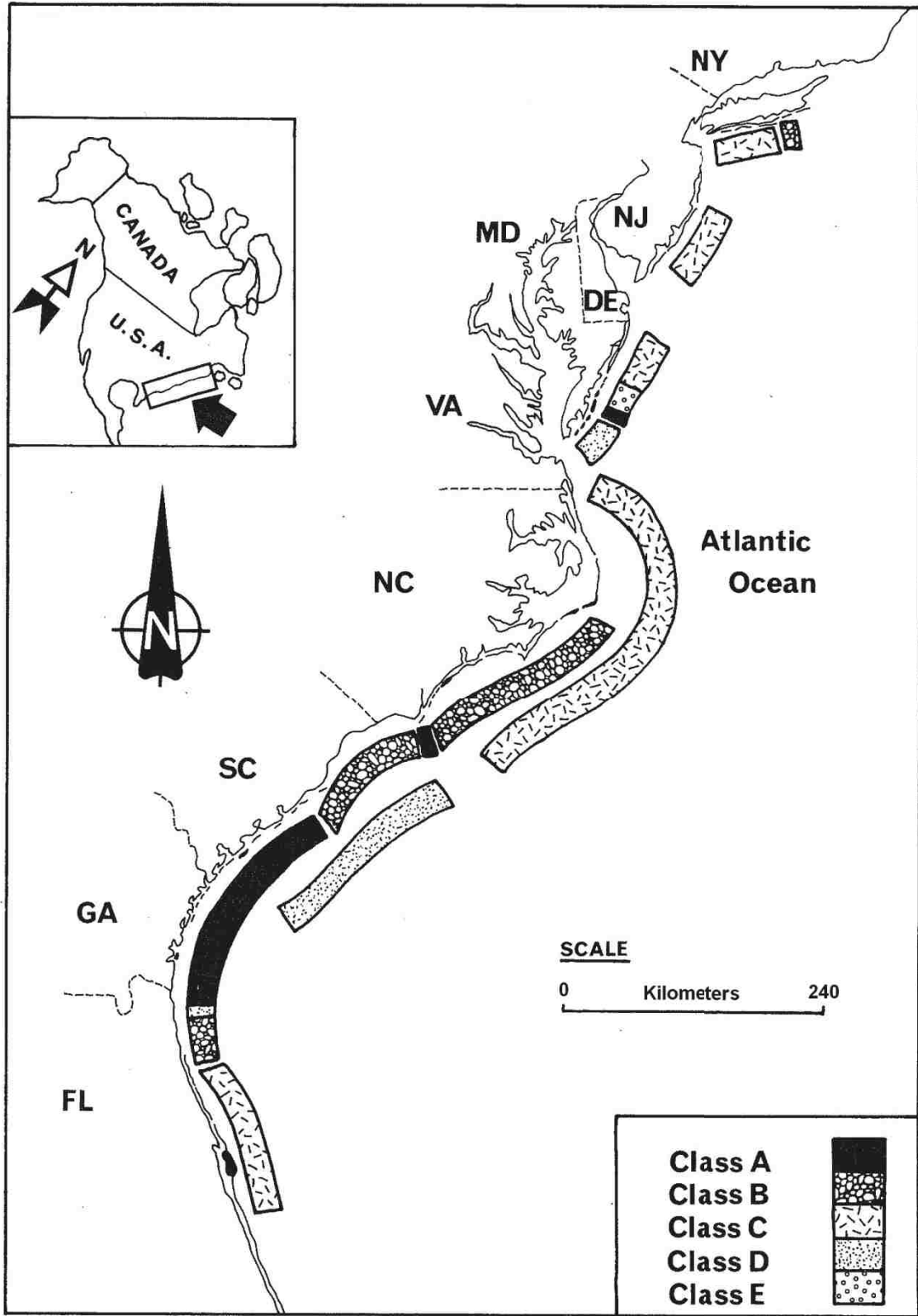


Figure 2.3. Williams and Leatherman's (1993) barrier island morphologies.

## CHAPTER THREE: METHODS

**Study area.** This study focused on the Holocene age barrier islands situated along the southeastern U.S. Atlantic coast from Florida to Maryland (**Figure 3.1**), the setting for classic textbook examples of barrier island morphologies (Davis, 1994). Prominent islands along this coastline stretch were identified using Google Earth. While aware of the subjectivity of selecting islands, omitting small islands might have enhanced the regional signal of wave and tidal energy across a maximum number of barrier islands. Fetch-limited barrier islands (Cooper et al., 2007) were not included, as they are often small in size and often landward of the fronting barrier landforms. Small islands surrounded by many inlets may also depart from more classical definitions of barrier islands (Oertel, 1985). I imported shoreline vector data by the National Oceanic and Atmospheric Administration (NOAA) to Google Earth to identify island outlines and verify shoreline position. The presence of prominent tidal inlets was often useful for island demarcation.

**Research question 1:** *What are the distinctive groupings of macroscale barrier island morphology?* The goal of this question was to compare the geographic distribution of older, more conceptual barrier island morphologic categories with those produced from a more recent quantitative classification. However, rather than fix on a final number of morphological groups, this classification seeks only to identify several possible robust hierarchical groupings of barrier island morphology.

**Barrier island classification data.** To perform the macroscale classification of barrier island morphologies, island mean width, length, mean width and length ratio, mean tidal range, mean wave height, orientation, and number of tropical storm/hurricane strikes were obtained for 77 islands (**Appendix A**). Using Google Earth, island mean width was measured approximately every 2 km perpendicular to the shoreline. Island length was measured parallel to the general orientation of each island. Tidal range and wave heights were obtained for each island using the US Geological Survey's Coastal Vulnerability Index database (Hammar-Klose and Thieler, 2001; Gornitz et al., 1994). A mean tidal range and a mean wave height were calculated for each island based on the average values of tidal range and wave height defined in segments that formed the perimeter of each individual island. Orientation was measured in degrees east from true

north along the same line that defined island length. These values were then relativized so that orientations on either side of north could be considered similar. Because tropical and extratropical storms can shape short-term barrier island evolution (Stone et al., 2004), the total number of tropical storms and hurricanes to make landfall on each island between 1851 and 2012 was derived from historical hurricane track data made available by NOAA Coastal Services (NOAA, 2014).

**Barrier island morphology classification.** Ward's method of hierarchical clustering based on Euclidian distances was used to classify barrier island morphologies. Since the island morphological variables were not directly comparable, they were Z-score standardized prior to clustering. The resulting dendrogram permitted the inference of several hierarchical levels at which barrier island morphologies could be grouped. The discriminatory power of the variables used to cluster observations typically peaks at some intermediate level of clustering. I used Indicator Species Analysis (ISA) to assess how well the macroscale variables discriminated among islands sites at different hierarchical levels. Although this procedure is designed to identify species that most discriminate among different sample sites in ecological studies, it can be used to characterize any indicator variable. In this way, ISA provides a measure of the robustness of a cluster solution. If final clusters are too finely divided then indicator values will be low. If final clusters are too large, then the internal heterogeneity will reduce the indicator values. Indicator values peak at some intermediate level of clustering (Dufrêne and Legendre, 1997). To visualize the relationships among these barrier island morphological clusters, I employed principal coordinate analysis (PCoA). PCoA is a distance-based, non-parametric ordination method. Euclidean distance was selected as the distance metric. Monte Carlo randomizations of the observed data were used to derive the significance of principal axes. PCoA and ISA were performed using PC-ORD statistical software package (McCune and Mefford, 1999).

**Research question 2:** *How do dune topographic types correspond to different clusters of barrier island morphology?* To address this question, it was first necessary to develop methods to characterize dune topographies. Variables from each of these methods were then assessed in ISA to determine how well each individual variable discriminated among barrier island macroscale morphologies. The most discriminatory variables in each method, as determined through ISA, were then combined into a single data set and

ordinated using PCoA to visualize a dune topographic state space. The results of this PCoA provided the means to examine how dune topographic types corresponded to island morphological types.

**Dune topography sampling and LIDAR mapping.** A representative island was selected from each of the macroscale clusters. Where possible, I selected islands that held some importance in the literature as sites of where research stations have been in operation. The dune topography of these islands was then linked to LIDAR ground data sets. LIDAR data were chosen as they are often used to derive high resolution representations of elevation for sandy coastal areas (Gares et al., 2006; Houser and Hamilton, 2009; Mitasova et al., 2010). LIDAR data sets were obtained from the NOAA Coastal Services Digital Coast website. The most recent LIDAR data sets available for each island that did not correspond to any immediate post-storm period were used. For the majority of sampled islands, this meant a 2010 data set collected by the U.S. Army Corps of Engineers. However, there were some exceptions to this rule. For South Core Banks and Parramore Island, post-Sandy LIDAR data sets collected in 2012 were used because data available for other recent years were unclassified (i.e. they were not processed to remove non-ground elevation points). All LIDAR processing was performed using the standard tools available in ArcGIS and a toolkit extension for processing LIDAR data called LAStools (Isenburg and Schewchuck, 2007).

**Area of interest (AOI) sites.** One meter digital orthophoto quarter quads (DOQQ) from the National Agricultural Imagery Program were used in conjunction with LIDAR data to identify and delineate three to four dune AOIs on each of the six islands. Each of these rectangular sites represented a predominant dune-beach morphology exhibited along each island (**Table 3.1**). The goal in selecting several sites was to capture the predominant range of dune topographies expressed along-shore.

Dune AOIs were not of uniform dimensions. Rather than try to force a standardization of any one size of an AOI, I used an adaptive sampling design where dune site characteristics determined the plot size. LIDAR point data corresponding to each of these rectangular AOIs were clipped out of the larger LIDAR data sets according to natural breaks in topography and vegetation. Since LIDAR data are often collected at low tide (Liu et al., 2007), the initial dimensions of each AOI extended from below the



waterline inland to the first occurrence of extensive dense woody vegetation or salt marsh. The distance from the waterline to non-dune vegetation was used as the length of the adjacent side of the AOI. Elevations for these square-shaped AOIs were then referenced to the mean high water (MHW) mark using NOAA's VDatum conversion program (Milbert, 2002; Stallins and Parker 2003). The MHW had to be adjusted manually for Parramore since the tidal conversion grid used in VDatum, which is based on observations made over the National Tidal Datum Epoch (1983 - 2001), could not take into account the recent rapid retreat of this island. All AOIs were then clipped along their lower edge to coincide with the MHW.

**Resampling and interpolation.** LIDAR point spacing among AOI sites sampled ranged from 0.59 to 1.39. Due to these variations in elevation point spacing between AOIs, LIDAR data were resampled to a uniform resolution as suggested by Su and Gibeaut (2010). Pilot analyses confirmed that a resolution of 1 meter was tenable for the resampling of LIDAR data. Because there were small patches of missing data in the resampling process due to vegetation obstructions or gaps in data collection, LIDAR data for each AOI were interpolated using an inverse distance weighing algorithm. These gaps typically spanned only a few meters at a maximum.

**Characterizing dune topography.** Three methods were developed to capture the topographic complexity of each AOI. No single method captured all the spatial characteristics of dunes. Descriptive statistics in the form of the frequency distribution of elevations provide a summary of the trends in elevation relative to the MHW. However, these data do not capture the spatial patterning of topography (i.e. the geometry of elevations). To capture the explicit spatial character of topography, I measured the spatial autocorrelation of elevation over a range of distances. These measurements were summarized in correlograms along a direction perpendicular to the shoreline. While this spatial measure of elevation captured the predominant elevational gradient of each AOI, it does not convey the multidirectional aspects of dune topography. To quantify how topography varied areally, as opposed to how it varied along a single direction, FRAGSTATS (McGarigal et al., 2012) landscape indices were used to quantify the landscape-scale pattern of patches defined by elevation. This allowed for an interpretation of patterns and processes associated with prominent dune building (linear

patches and fine resolution differentiation of elevations) and overwash (circular patch shapes and more aggregated elevations).

**Descriptive statistics.** Descriptive statistics for elevation are often used in before and after studies of hurricane impacts on dunes since they are essentially comparisons of elevation based on a common datum (FitzGerald et al., 2008; Magliocca et al., 2011). For resampled data for each AOI, a frequency distribution of elevations was used to derive the mean, minimum, maximum, kurtosis, skewness, and the interquartile range.

**Correlograms.** Resampled LIDAR point information for each AOI were imported into GS+ software (Robertson, 2000) as X, Y, and Z data for spatial autocorrelation analysis. Moran's I, a common measure of spatial autocorrelation (Legendre, 1993), was calculated at 1 meter distance classes in the direction perpendicular to the shoreline. These distance classes ranged up to the maximum length of the AOI. Moran's I generally ranges from -1 to 1, with negative values indicating increasing elevational contrasts while positive values indicate elevations that are similar.

**Landscape indices.** FRAGSTATS was used to generate spatial metrics that incorporate geometric landscape patterns (McGarigal et al., 2012). Although FRAGSTATS is designed to work with categorical data, I employed a reclassification of rasterized LIDAR data for each AOI to convert elevations to a more categorical representation. This was done by creating a 1 meter resolution digital elevation model (DEM), multiplying the existing elevation in each raster grid cell by 10, and then converting each resulting value to an integer. This reduced the number of unique elevation observations that defined the continuous surface of each AOI raster to a smaller set. For example, given a large number of unique raster elevations for an AOI, ranging from 4.23 to 0.05 meters for example, the employed reclassification would result in a range of 42 to 5, or 4.2 to .5 meters. This decreased the number of elevation classes from one based on all the possible centimeter intervals between 4.23 and 0.05 (essentially a continuous surface representation), to one based on all decimeter intervals between 4.2 and 0.5 (a more categorically-oriented representation).

To avoid the indiscriminate computation of landscape indices in FRAGSTATS without regard to their process interpretation (Kupfer, 2012), I judiciously selected a set of

FRAGSTATS indices to measure for each raster AOI. Cushman et al. (2008) recommended a set of eight consistently discriminating landscape FRAGSTATS indices. I used these recommended indices to narrow down the pool of possible indices. I also based the selection of indices on recommendations as to which are useful for characterizing continuous surfaces, as developed in the field of surface metrology (McGarigal et al., 2009). Indices were also constrained to those that could be interpreted as relevant for discerning landscape processes related to overwash and dune building.

The variables chosen were the landscape shape index (LSI), contagion (CONTAG), perimeter-area fractal dimension (PAFRAC), area-weighted mean shape index (SHAPE\_AM), aggregation index (AI), interspersion and juxtaposition index (IJI), largest patch index (LPI), and Simpson's patch diversity index (SIDI). LSI measures the perimeter-to-area ratio, an indicator of the general geometric complexity of the landscape. The value ranges from 1 to infinity. When the landscape is regular in shape it is equal to 1 and this value increases with increasing landscape shape irregularity. CONTAG is a measure of clumpiness. It equals 0 when cells of different patch types are disaggregated and interspersed within a landscape. The value increases as cells of the same patch type become aggregated and equals 100 when they are maximally aggregated. IJI is similar to CONTAG in that it measures clumpiness, but it does this on patches instead of cells. When a patch of a certain type is adjacent to only one other patch type, the value is equal to 0. The value increases to 100, where patch types are equally adjacent to other patch types. LPI equals the percent of the landscape that the largest patch comprises. LPI approaches 0 when the largest patch in the landscape is increasingly small. It equals 100 when the largest patch comprises 100% of the landscape. SIDI is a measure of landscape patch diversity. It equals 0 when the landscape only has one patch type and equals 1 when patch diversity increases and each of the patches are equally expressed across the landscape. AI measures how similar patch neighbors are to each other. It equals 0 when the patch types are maximally disaggregated (i.e. when there are no like adjacencies); AI increases as the patches within a landscape become increasingly aggregated and equals 100 when the landscape consists of a single patch. PAFRAC is a measure of patch shape complexity defined by perimeter-area relationships. If the small and large patches of elevation have simple, geometric shapes then PAFRAC will be low. If small and large patches have more complex shapes, patch perimeter increases more rapidly as patch area increases,

and PAFRAC will increase. SHAPE\_AM is another measure of patch shape complexity. It is an area weighted index that approaches a value of 1 when the elevation patches are square-like, and increases without limit as patch shape becomes more irregular.

**Comparing dune topographies.** ISA was used to identify the discriminatory FRAGSTATS indices and the descriptive statistics summarizing elevation. It was also used to identify at what hierarchical level of island morphologic clustering the discriminatory effectiveness of these dune variables peaked. ISA also performs a Monte Carlo randomization of the significance of all indicator values (IV). The IV provides an assessment of the robustness of observed dune variables by comparing it to the values calculated from a randomization of the data. The most discriminatory variables, those with the highest indicator values and statistical significance, were then combined with correlogram distance class variables so that they could be jointly visualized with PCoA and interpreted through correlations with significant axes. This final visualization allowed us to characterize the dune topographies underlying the different barrier island morphologies. Where necessary, dune metrics were transformed to Z-scores to facilitate comparisons of variables that were not directly comparable.

**Table 3.1.** Description of island sites sampled.

| Island         | Site | Process-form description   |
|----------------|------|--|
| Parramore      | A    | Active overwash into saltmarsh.  |
|                | B    | Active overwash into thin strip of maritime forest.                    |
|                | C    | Active overwash, formation of Parramore pimples.                       |
|                | D    | Active, broad overwash.  |
| Bull           | A    | Evidence of overwash near inlet.                                       |
|                | B    | Wide, persistent overwash into salt marsh.                             |
|                | C    | Narrow dune, highly erosional.   |
|                | D    | Dune ridging, accretional.   |
| Sapelo         | A    | Wide dune area, ridging, accretional.                                  |
|                | B    | Narrow, erosional.   |
|                | C    | Accretional with ridging.  |
| Kiawah         | A    | Active overwash.   |
|                | B    | Some dune ridges, human impacts, accretional.                          |
|                | C    | Narrower, erosional.   |
|                | D    | Wide (multiple ridges), accretional.                                   |
| S. Core Banks  | A    | Narrower, negative relief, ample and active overwash.                  |
|                | B    | Overwashed but with wider vegetated plane.                             |
|                | C    | Wide vegetated dune area, more accretion.                              |
| Cape Canaveral | A    | Narrow and single, densely vegetated dune ridge.                       |
|                | B    | Narrower, clumpier vegetation patches, evidence for historic overwash. |
|                | C    | Wide dune area, patchy vegetation.                                     |
|                | D    | Wide, multiple dune ridges, accretional.                               |

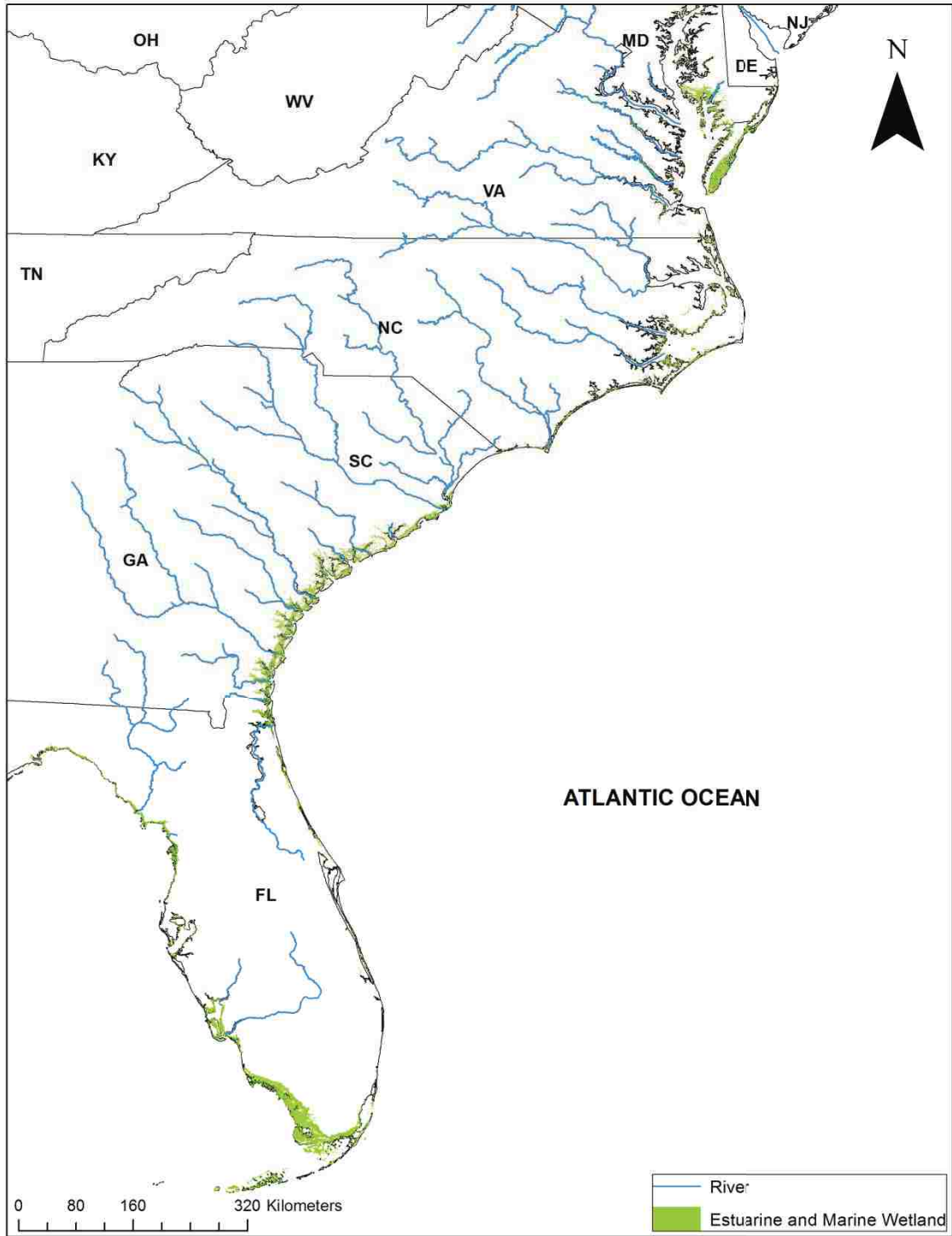


**Figure 3.1.** Study area.

## CHAPTER FOUR: RESULTS

**Barrier island macroscale morphology.** ISA indicated that the grouping of barrier islands into 5, 6, or 7 clusters were similarly strong (**Table 4.1**). However, a grouping of 7 barrier island clusters was selected to initialize the stepwise (7, 6, 5, 4...) comparison of dunes from different island morphologic clusters (**Figure 4.1**). PCoA arranged these islands along orthogonal axes that had significant correlations with the macroscale variables (**Table 4.2 and Figure 4.2**). Approximately 47% of the variance ( $p = 0.001$ ) is explained by the first axis and 22% of the variance ( $p = 0.002$ ) is explained by the second axis.

The general distribution of all of these clusters had some correspondence to the broad tidal and wave regimes that demarcate the Georgia Bight (**Figure 4.3**). However, some sections of the coast were more heterogeneous, with less consistency along the coast in which barrier island morphology was expressed. Cluster 1 islands are all Florida islands located along the southernmost section of this state. They all have extensive development and many of the beaches are likely engineered to a degree through renourishment. Cluster 2 islands are the greatest in number and are predominantly located along cusped coastlines in South Carolina, North Carolina, and Virginia. This cluster developed north of the coastal areas where low wave energy and estuaries permit the development of extensive salt marshes. Group 3 islands are found mostly in Florida and southernmost Georgia with a small occurrence in South Carolina. These more heterogeneously shaped islands are notably of greater widths than other clusters (**Table 4.3**). They responded most strongly to the width gradient expressed on the second axis in the PCoA. Group 4 islands represent the classic Sea Islands of the Georgia and southernmost South Carolina coast. They form a tight cluster aligned along the second axis in the PCoA scatterplot. Like Cluster 2, Group 5 islands occur along cusped shorelines in South Carolina and North Carolina. These islands have more mesotidal shapes but extend into higher wave energy environments to the north, and like Cluster 2, can experience overwash. They tend to have more welded island morphologies, shorter lengths, and orientations that are more east-west. Group 6 islands appear in mid-coast Florida and in North Carolina and Virginia. They tend to have longer island morphologies, but island retreat has resulted in locations close to the mainland.

Group 7 islands were exceptionally long islands comprising cusped forelands in North Carolina and Florida.

**Dune topographies.** Representative islands from six of the seven clusters were chosen for the development of dune metrics. The cluster group comprising of islands in southern Florida (cluster group 1) was not considered in this part of the study due to the high level of human impact found on these islands (**Table 4.4**). In some cases, the beaches were so narrow on the aerial imagery as to preclude dune site detection. The following islands were selected:

Parramore Island (cluster group 2) is a transgressive, tidal-dominated barrier located on the Delmarva Peninsula off the coast of Virginia (**Figure 4.4a**). It is approximately 10 km long and is drumstick in shape with a wide northern end and a slightly narrower southern end. It is separated from neighboring islands by the presence of large tidal-ebb deltas. The dune line in the northern end of the island has high dune topography and it decreases to the south in tandem with increasing overwash. Currently, Parramore is rapidly retreating towards the mainland (short term rates of retreat 2.7 m/year) (Davis, 1994; Richardson and McBride, 2007).

South Core Banks (cluster group 3) is a transgressive, wave-dominated barrier located on the coast of North Carolina (**Figure 4.4b**). At 36 km in length, it is the most extensive of the three islands that make up the Core Banks island chain. The northern end of South Core is narrow and widens as you go south, forming a hook-like feature known as Cape Lookout. Due to its geographic location and orientation, the island has a long history of hurricane and tropical storm impacts. Overwash, particularly in the northernmost section, contributes to the island's low-profile (Davis, 1994; Stallins and Parker, 2003; Riggs, 2007).

Bull Island (cluster group 4) is a mixed-energy (tide-dominated) barrier located on the coast of South Carolina north of Charleston (**Figure 4.4c**). This island is relatively short and has an approximate length of 9 km. It is drumstick in shape with a wide northern end and a considerably narrower southern end. Due to its position along the coastline, it experiences little direct hurricane impacts compared to South Core Banks. Dune



features occur toward the north and decrease going south (Davis, 1994; Hayes and Michel, 2008).

Kiawah Island (cluster group 5) is a mixed-energy (tide-dominated) barrier located on the coast of South Carolina south of Charleston (**Figure 4.4d**). The island is approximately 15 km in length and closely resembles Bull Island in shape. Like Bull Island, it receives little direct hurricane influence (Hayes and Michel, 2008), although it has much more human impacts than Bull Island.

Sapelo Island (cluster group 6) is a mixed-energy (tide-dominated) barrier located on the coast of Georgia (**Figure 4.4e**). Sapelo is actually the Holocene fringing island that has welded to the Pleistocene core that is often identified as Sapelo. It is approximately 8 km in length. Like the other Sea Islands off the Georgia coast, it has experienced little tropical storm and hurricane influence. Sediment dynamics on Sapelo are influenced by the adjacent large tidal inlets and extensive marsh development (Davis, 1994; Stallins and Parker, 2003).

Cape Canaveral (cluster group 7) is a wave-dominated barrier located on the central coast of Florida (**Figure 4.4f**). The island is approximately 80 km in length and welded against the Florida mainland. The northern end of Cape Canaveral is narrow and widens considerably to form the Canaveral Peninsula (Davis, 1994).

**Dune metrics for individual island sites.** The frequency distribution of elevation data did not converge on a single elevational profile for all islands (**Figure 4.5 and Appendix B**). The largest range in elevation values among sites were found on Core Banks and Cape Canaveral and the lowest on Parramore. The range of elevations on Bull, Sapelo and Kiawah were similar and fell above the range of values found on Parramore. Correlograms also varied among islands and sites. Some islands had more variable correlograms from site to site, notably Bull, Sapelo, Kiawah and Cape Canaveral (**Figure 4.6**). The reclassified AOI rasters used for FRAGSTATS conveyed a range of patterns (**Figure 4.7 and Appendix C**), from more linear topographic trends to more circular patch structure. The diversity of topographies among sites was also variable from island to island. Parramore conveyed a less linear simplified topography. Bull, Sapelo, and Kiawah had more diverse, complex patterns of topography. South Core Banks and Cape

Canaveral had more consistent along-island patch structure, but they differed in their degree of linearity.

Shifts in the strength of ISA indicator values and their Monte Carlo-derived significance peaked when islands were grouped into three clusters (**Table 4.5**). ISA indicated that the mean, maximum, mode (50<sup>th</sup> percentile) and the 25<sup>th</sup> and 75<sup>th</sup> percentile elevation were the statistically significant descriptive variables at this hierarchical division. PAFRAC, SHAPE\_AM, and AI were the most significant FRAGSTATS variables. Because the spatial autocorrelation characterization only produced univariate descriptors, Moran's I at different distance classes could not be directly assessed through ISA. A PCoA of the spatial autocorrelation data was used to inspect the degree these data discriminated among islands. The first two axes of the PCoA solution were significant based on Monte Carlo randomizations of the data and extracted 74% of the variance (Axis 1 = 63%,  $p = 0.001$ ; Axis 2 = 12%,  $p = 0.001$ ; **Figure 4.8**). As seen in Figure 4.6, island sites along to the right of Axis 1 tend to have Moran's I values that continue to fall off and become strongly negative with distance inland. Island sites to the left of Axis 2 tend to have Moran's I values that fluctuate and rise back up and often move around low positive and negative values. This pattern repeats along the second axis. Island sites at the top of the plot have correlograms with Moran's I values that drop off with increasing distance but then tend to come back up toward zero and fluctuate around this dividing point.

**PCoA of dune metrics.** The descriptive statistics with the strongest indicator values (mean, maximum, mode, 25<sup>th</sup> percentile, and 75<sup>th</sup> percentile elevations) and the FRAGSTATS indices with the strongest indicator values (PAFRAC, SHAPE\_AM, and AI) were combined with the X and Y coordinates derived from PCoA of the spatial autocorrelation data and visualized with PCoA (**Figure 4.9**). The first two axes were determined to be significant based on Monte Carlo tests of the observed versus randomized data ( $p < 0.05$ ). The first axis captured 59.2% of the variance. The second axis captured 20.6% of the variance. Thus, this final PCoA of the discriminatory dune metric variables captured approximately 80% of the variability among the dune topographies for the AOIs. Island sites formed two domains or regions in the scatterplot, largely separated along the second axis. The upper domain consisted largely (but not exclusively) of sites from Bull, Sapelo, and Kiawah. The lower domain consisted mostly of sites from Cape Canaveral, South Core Banks, and Parramore. However, in each

domain there were island sites from the other domains. The sites that jumped away from their predominant domains were Parramore B, Sapelo C, and Kiawah B.

Correlations of axis scores with the original dune variable provided a pattern-process interpretation for how sites were arranged. The aggregation index, AI, loads strongly on the first axis (**Figure 4.10a**). It increases toward island sites with more overwash, and more uniform topographies consisting of larger patches of similar ranged elevations (see Figure 4.7). Since PAFRAC captures the fractal dimension of a landscape, its variation is suggestive of differences in the underlying pattern-generating process. PAFRAC separated out island sites primarily along the first axis (**Figure 4.10b**). PAFRAC increases on islands that are higher and less prone to overwash. It decreases for Parramore sites A through C given their flat topographies, more frequent overwash, and less complex patch shapes. SHAPE\_AM illustrated differences in topography in agreement with PAFRAC and AI. It also differentiated island sites primarily on the first axis (**Figure 4.11a**). Locations that were lower and more susceptible to overwash had more irregular patch shapes and higher SHAPE\_AM values. On higher elevation sites, and where overwash was less frequent, patches were more rectangular in shape and affiliated with more intact, rectilinear dunes and swales.

The descriptive elevational variables in the final PCoA produced similarly high loadings on the first axis. Mean elevation above the MHW had the highest individual correlation (**Figure 4.11b**). The pattern of mean elevations among island sites corroborated the pattern-process interpretation of the FRAGSTATS metrics. Lower elevation sites had higher AI values (more aggregated elevation values), smaller PAFRAC (a changing fractal dimension), and larger SHAPE\_AM values (a shift from rectangular patch shapes to more convoluted circular shapes). The greatest elevational contrasts, those between Cape Canaveral and Parramore, were expressed along the first axis. Cape Canaveral has some of the highest dune elevations among all islands, while Parramore is low and rapidly retreating landward.

The only variable to load significantly on the second axis was the spatial autocorrelation distance class variable data ( $r = 0.80$ ), specifically, the first axis coordinates (X) from the PCoA of the spatial autocorrelation data (**Figure 4.12**). It is along this second axis that a prominent break develops between the two main domains of dunes. Because the spatial

autocorrelation values have been reduced into X and Y coordinates, it is difficult to ascertain a more process-based interpretation of the data. Also, only 20% of the variance in the data is embedded in the second axis. However, there is a propensity for more of the island sites in the top domain to have Moran's I values in the correlogram that fluctuate around zero after initially dropping off with increasing distance. Island sites at the bottom tend to have increasing negative values of Moran's I with distance.

**Table 4.1.** Indicator Values (IV) and associated p-values for 5, 6, and 7 macroscale groupings derived from Indicator Species Analysis on macroscale variables.

| Variable    | 5            | 6            | 7            |
|-------------|--------------|--------------|--------------|
| Length      | 0.64, 0.0002 | 0.60, 0.0004 | 0.57, 0.0002 |
| Width       | 0.60, 0.0002 | 0.56, 0.0002 | 0.53, 0.0002 |
| Hurricanes  | 0.59, 0.0002 | 0.56, 0.0004 | 0.53, 0.0008 |
| Tidal Range | 0.53, 0.0002 | 0.49, 0.0002 | 0.46, 0.0004 |
| Wave Height | 0.39, 0.1034 | 0.37, 0.1018 | 0.34, 0.1016 |
| LW Ratio    | 0.55, 0.0020 | 0.52, 0.0004 | 0.49, 0.0010 |
| Orientation | 0.42, 0.0644 | 0.39, 0.0634 | 0.39, 0.0052 |
| Average     | 0.53, 0.0244 | 0.50, 0.0238 | 0.47, 0.0156 |

**Table 4.2.** Spearman’s correlation analysis between original island macroscale variables and PCoA axis scores.

| Island Variable       | Axis 1   | Axis 2   |
|-----------------------|----------|----------|
| Length                | -0.777** | 0.063    |
| Mean width            | -0.141   | 0.836**  |
| Length to width ratio | -0.613** | -0.679** |
| Hurricane strikes     | -0.670** | 0.285*   |
| Mean tidal range      | 0.703**  | 0.462**  |
| Mean wave height      | -0.625** | 0.060    |
| Orientation           | -0.570** | 0.300**  |

\*p < .05; \*\*p < .001

**Table 4.3.** Macroscale island cluster summary.

|           | Average and Standard Deviation (SD) for island variables |            |                               |                 |                 |             |                       |
|-----------|--|------------|-------------------------------|-----------------|-----------------|-------------|-----------------------|
|           | Length (Km)  | Width (Km) | Hurricane Strikes (1851-2012) | Tidal Range (m) | Wave Height (m) | LW Ratio    | Orientation (Degrees) |
| Cluster 1 | 17.2 ± 6.6   | 0.7 ± 0.4  | 5.0 ± 2.5                     | 0.7 ± 0.1       | 1.0 ± 0.1       | 33.1 ± 24.2 | 2                     |
| Cluster 2 | 10.1 ± 6.5   | 0.3 ± 0.1  | 2.1 ± 1.7                     | 1.2 ± 0.2       | 1.1 ± 0.1       | 43.2 ± 20.3 | 29.4                  |
| Cluster 3 | 20.0 ± 15.0  | 1.9 ± 1    | 6.1 ± 3.6                     | 1.6 ± 0.3       | 1.1 ± 0.1       | 10.3 ± 5.5  | 12                    |
| Cluster 4 | 9.4 ± 3.8  | 0.8 ± 0.4  | 3.9 ± 1.3                     | 2.1 ± 0.1       | 1.0 ± 0.1       | 16.4 ± 10.9 | 30.2                  |
| Cluster 5 | 10.6 ± 8.9   | 0.5 ± 0.2  | 3.6 ± 3.8                     | 1.4 ± 0.2       | 1.1 ± 0.1       | 21.9 ± 14.9 | 70.9                  |
| Cluster 6 | 43.1 ± 13.1  | 0.6 ± 0.3  | 10.1 ± 2.9                    | 0.8 ± 0.3       | 1.2 ± 0.1       | 88.0 ± 41.5 | 10                    |
| Cluster 7 | 87.0 ± 16.7  | 1.0 ± 0.2  | 27.0 ± 10.9                   | 0.8 ± 0.1       | 1.3 ± 0.1       | 92.0 ± 23.4 | 343                   |

**Table 4.4.** Islands for each of the clusters as derived from PCoA and hierarchical and agglomerative clustering.

| Cluster | Members   |
|---------|---|
| 1       | Highland Beach (FL), Hillsboro Beach (FL), Key Biscayne (FL), Lauderdale-by-the Sea (FL), Miami Beach (FL), Palm Beach (FL), Singer Island (FL), Sunny Isle (FL)  |
| 2       | Cape Island (SC), Cedar Island (SC), Collins Island (SC), Debidue Island (SC), Murphy Island (SC), Pawleys Island (SC), Sand Island (SC), Figure Eight Island (NC), Harbor Island (NC), Masonboro Island (NC), Ocracoke Island (NC), Onslow Beach (NC), Portsmouth Island (NC), Assawoman Island (VA), Cedar Island (VA), Cobb Island (VA), Hog Island (VA), Metompkin Island (VA), Myrtle Island (VA), Parramore Island (VA), Ship Shoal Island (VA), Smith Island (VA), Wreck Island (VA) |
| 3       | Amelia Island (FL), Anastasia Island (FL), Jacksonville Beach (FL), Little Talbot Island (FL), Cumberland Island (GA), Bull Island (SC), Hilton Head Island (SC), Bald Head Island (NC), Pleasure Island (NC)   |
| 4       | Blackbeard Island (GA), Jekyll Island (GA), Little Tybee Island (GA), Ossabaw Island (GA), St. Catherines Island (GA), Sapelo Island (GA), Sea Island (GA), Tybee Island (GA), Wassaw Island (GA), Fripp Island (SC)  |
| 5       | Capers Island (SC), Edings Island (SC), Folly Island (SC), Isle of Palms (SC), Kiawah Island (SC), Lighthouse Island (SC), Sullivans Island (SC), Waties Island (SC), Bear Island (NC), Bird Island (NC), Bogue Banks (NC), Browns Island (NC), Holden Beach (NC), Oak Island (NC), Ocean Isle Beach (NC), Shackleford Banks (NC)   |
| 6       | Hutchinson Island (FL), Jupiter Island (FL), North Hutchinson Island (FL), Sebastian Island (FL), Core Banks (NC), Topsail (NC), Assateague Island (MD)   |
| 7       | Cape Canaveral (FL), Ormond Beach (FL), Currituck Banks (NC), Hatteras Island (NC)  |



**Table 4.5.** Indicator Values (IV) and associated p-values for 2, 3, 4, 5, and 6 macroscale groupings derived from Indicator Species Analysis on dune topographic variables.

|                            | 2            | 3                   | 4            | 5            | 6            |
|----------------------------|--------------|---------------------|--------------|--------------|--------------|
| <b><u>Descriptives</u></b> |              |                     |              |              |              |
| <b>Mean</b>                | 61.8 (0.002) | <b>46.0 (0.001)</b> | 36.1 (0.004) | 30.1 (0.010) | 25.2 (0.024) |
| Minimum                    | 51.8 (0.473) | 36.0 (0.359)        | 28.5 (0.165) | 23.0 (0.258) | 19.6 (0.209) |
| <b>Maximum</b>             | 60.6 (0.002) | <b>45.9 (0.001)</b> | 34.9 (0.003) | 27.8 (0.022) | 23.2 (0.046) |
| Skewness                   | 55.6 (0.428) | 45.8 (0.087)        | 37.8 (0.060) | 31.3 (0.098) | 25.8 (0.204) |
| Kurtosis                   | 54.5 (0.544) | 40.9 (0.424)        | 32.1 (0.482) | 25.0 (0.768) | 21.1 (0.860) |
| <b>25<sup>th</sup> %</b>   | 65.1 (0.008) | <b>49.9 (0.003)</b> | 39.7 (0.007) | 31.2 (0.047) | 26.4 (0.075) |
| <b>50th (Mode)</b>         | 61.3 (0.003) | <b>44.9 (0.007)</b> | 35.5 (0.008) | 28.7 (0.035) | 24.0 (0.072) |
| <b>75<sup>th</sup> %</b>   | 60.6 (0.005) | <b>44.6 (0.005)</b> | 35.0 (0.006) | 29.6 (0.010) | 24.6 (0.027) |
| Average IV                 | 58.9 (0.183) | 44.2 (0.111)        | 34.9 (0.092) | 28.3 (0.156) | 23.8 (0.190) |
| Randomized IV              | 0.0038       | <b>0.0002</b>       | 0.0008       | 0.0144       | 0.0416       |
| <b><u>FRAGSTATS</u></b>    |              |                     |              |              |              |
| LPI                        | 51.6 (0.488) | 35.4 (0.507)        | 26.7 (0.689) | 21.6 (0.780) | 18.2 (0.836) |
| LSI                        | 53.4 (0.142) | 37.2 (0.122)        | 28.0 (0.256) | 22.6 (0.368) | 18.8 (0.522) |
| <b>SHAPE_AM</b>            | 50.7 (0.751) | <b>40.0 (0.003)</b> | 30.9 (0.004) | 24.8 (0.021) | 21.1 (0.022) |
| CONTAG                     | 51.8 (0.455) | 36.0 (0.352)        | 27.6 (0.362) | 23.5 (0.086) | 20.1 (0.048) |
| IJI                        | 51.7 (0.472) | 36.8 (0.175)        | 27.2 (0.478) | 22.1 (0.554) | 20.4 (0.065) |
| SIDI                       | 54.5 (0.051) | 37.9 (0.045)        | 29.0 (0.065) | 23.3 (0.142) | 19.3 (0.297) |
| <b>PAFRAC</b>              | 50.8 (0.727) | <b>38.9 (0.010)</b> | 28.0 (0.209) | 22.2 (0.479) | 19.4 (0.188) |
| <b>AI</b>                  | 51.5 (0.528) | <b>40.7 (0.000)</b> | 31.3 (0.001) | 25.2 (0.005) | 21.5 (0.007) |
| Average IV                 | 52.0 (0.452) | 37.9 (0.152)        | 28.6 (0.258) | 23.2 (0.304) | 19.9 (0.248) |
| Randomized IV              | 0.3625       | <b>0.0036</b>       | 0.0198       | 0.0490       | 0.0190       |

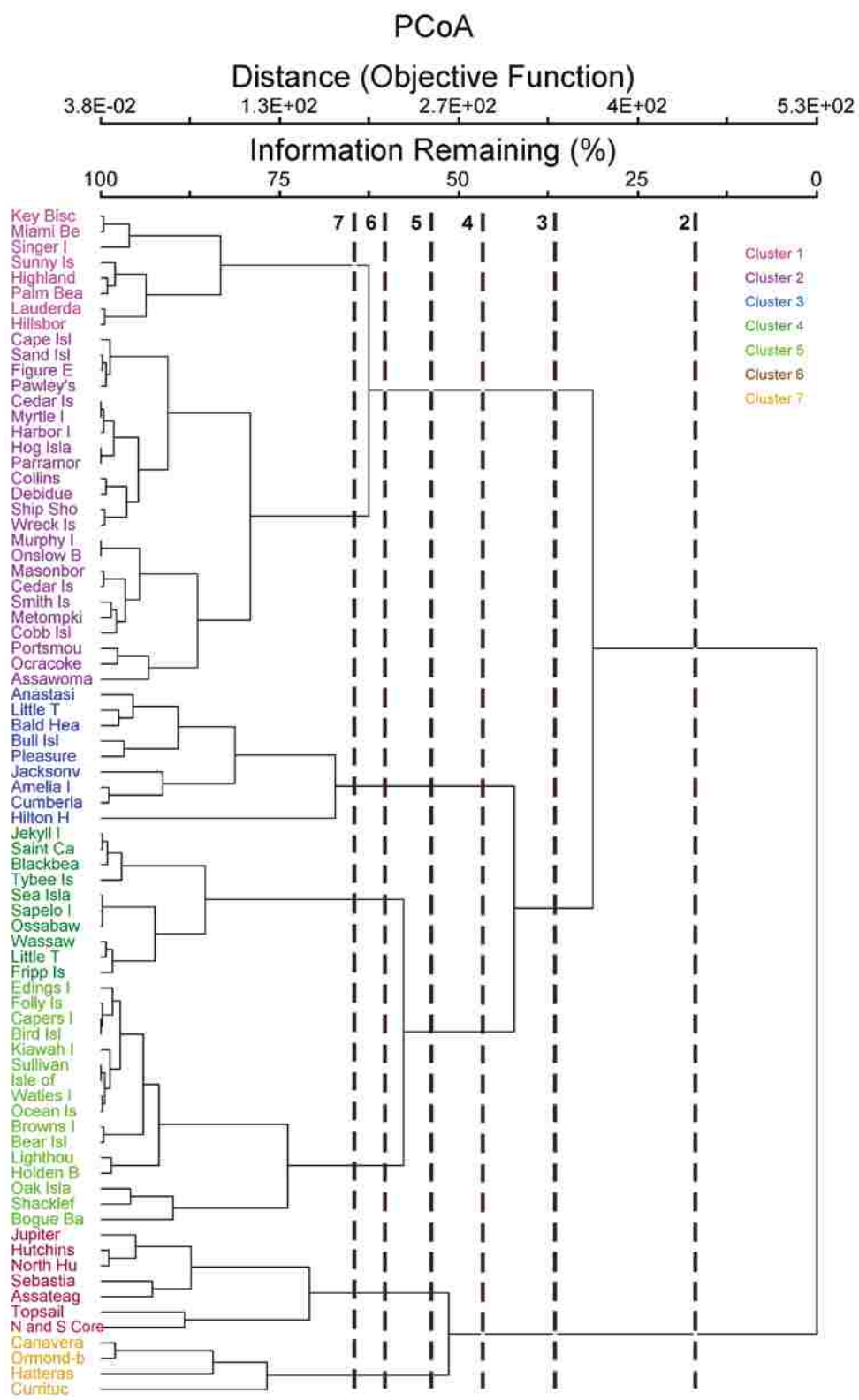


**Figure 4.1.** Cluster dendrogram of major barrier island morphologic groups. Dashed lines indicate hierarchical divisions into 2, 3, 4, 5, 6, and 7 barrier island groupings.

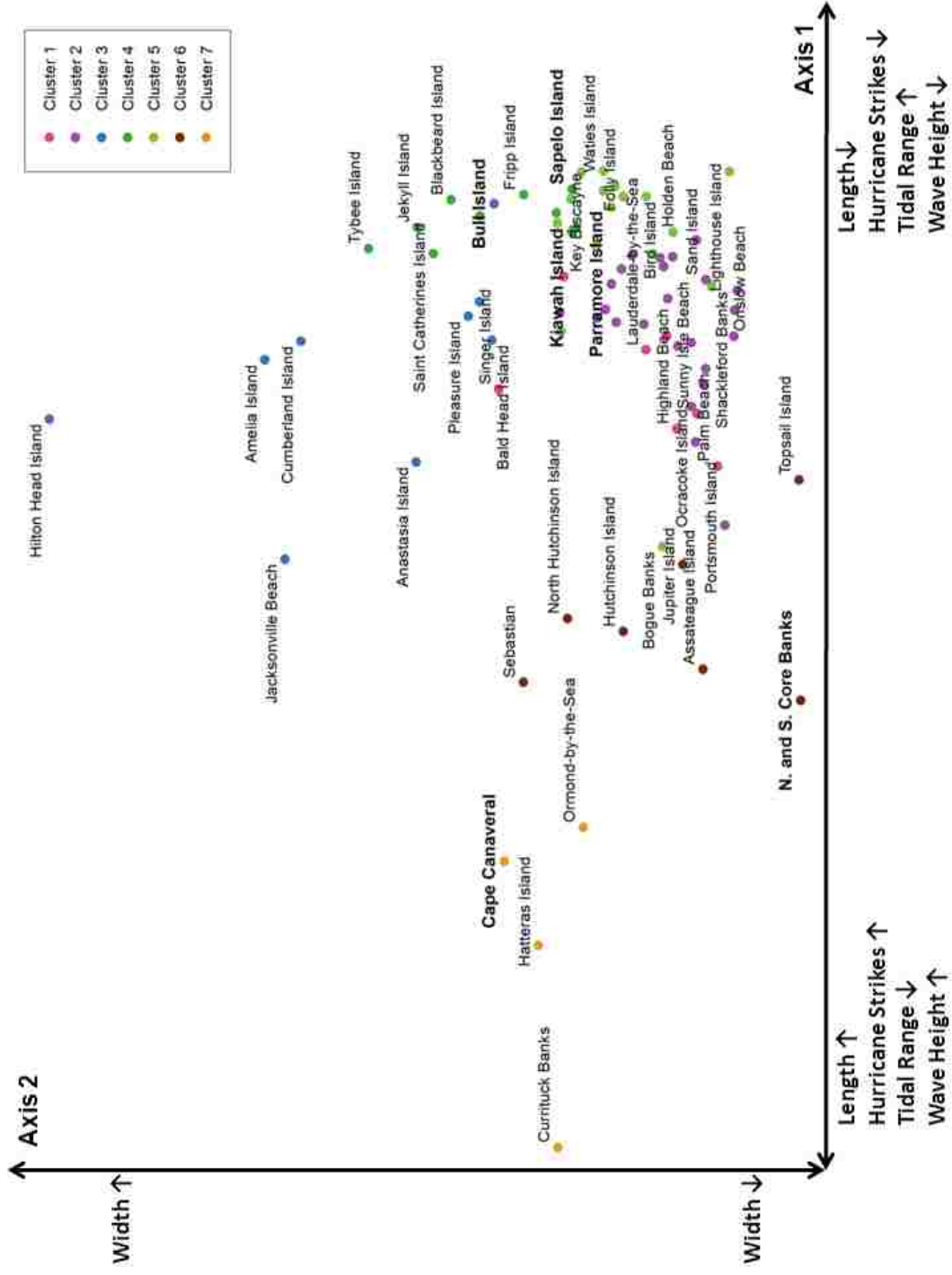
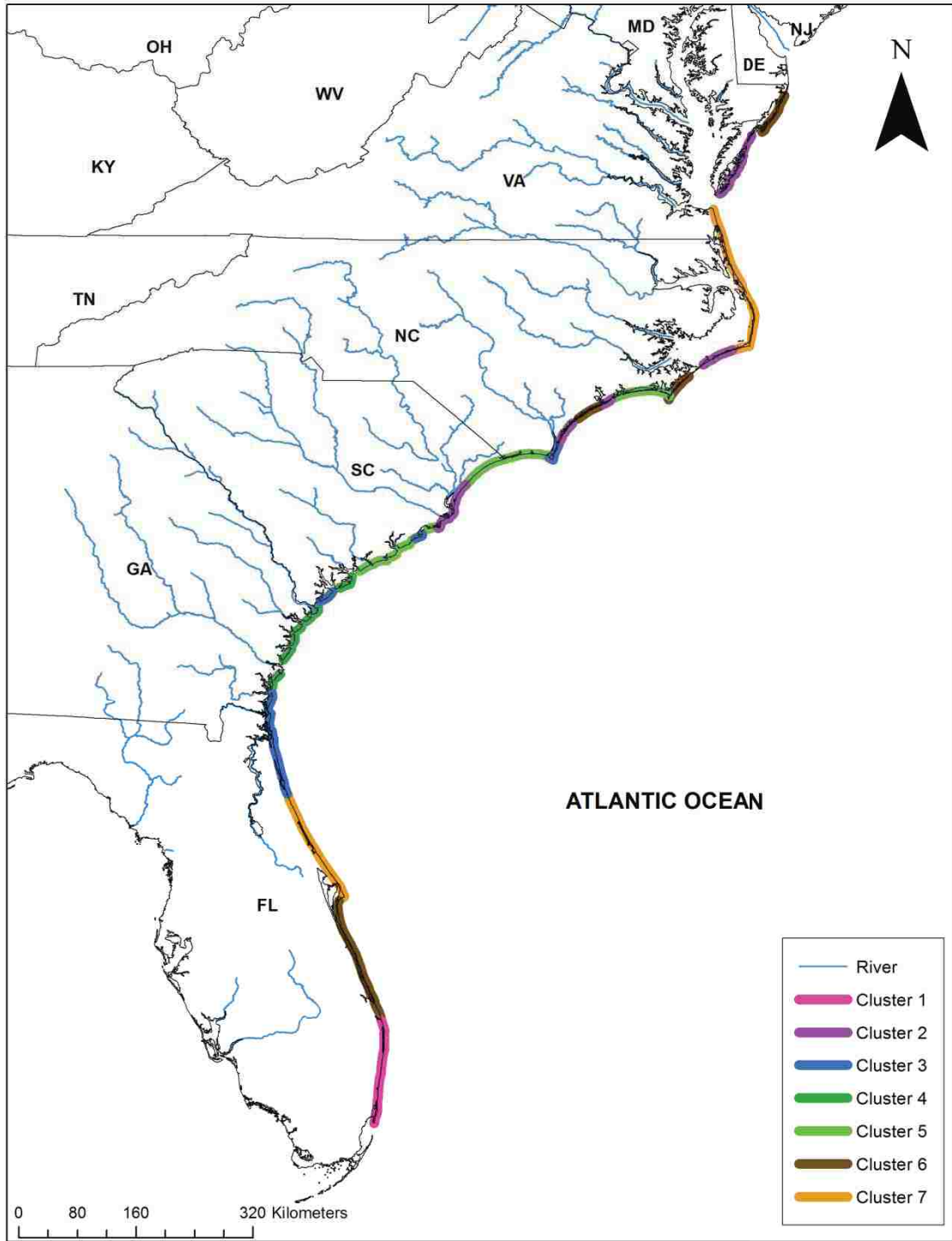
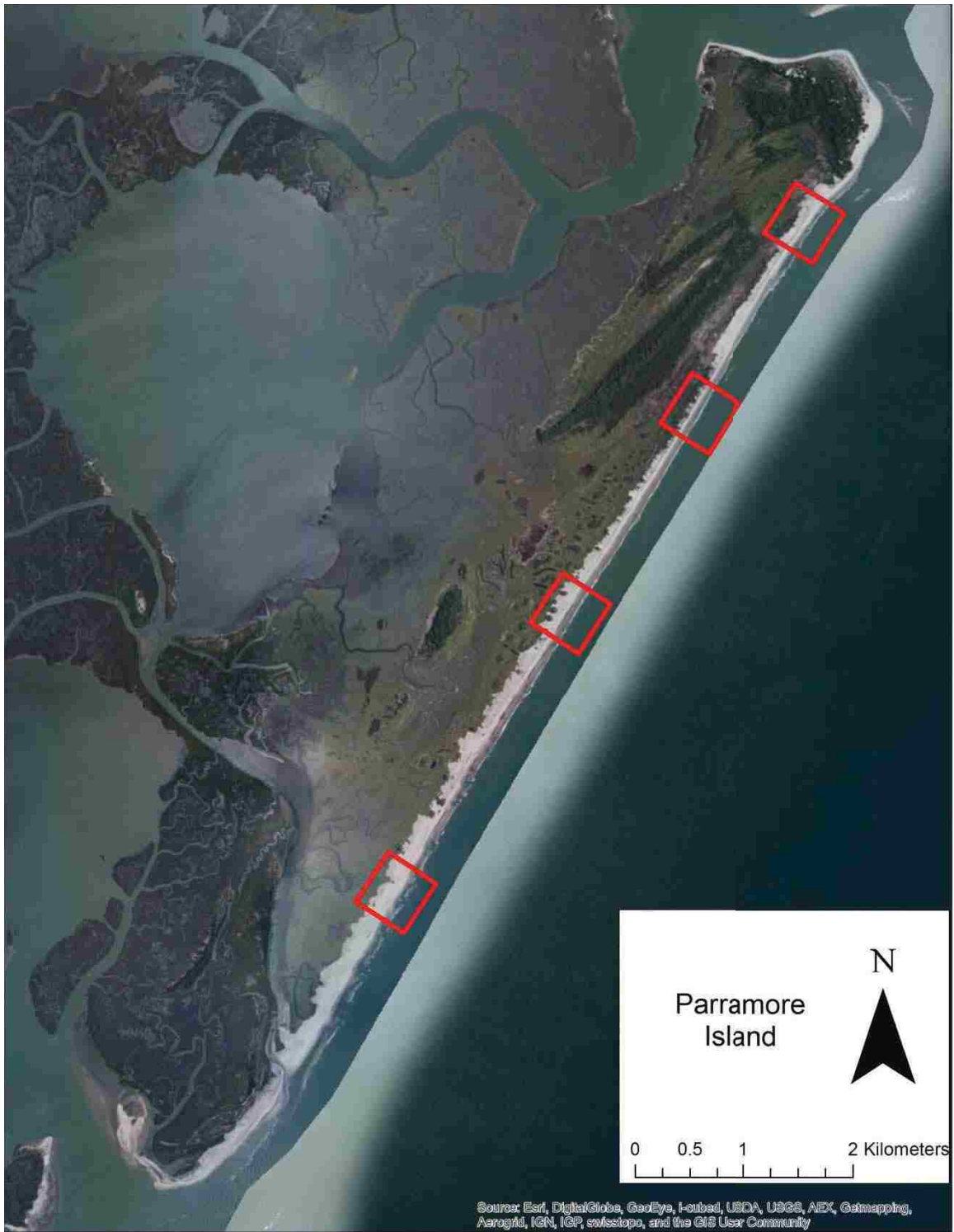


Figure 4.2. PCoA ordination of barrier island macroscale variables.



**Figure 4.3.** Distribution of island clusters along the coastline.



**Figure 4.4a.** Parramore Island, Cluster 2, and AOIs (in red).



**Figure 4.4b.** South Core Banks, Cluster 3, and AOIs (in red).



Figure 4.4c. Bull Island, Cluster 4, and AOIs (in red)



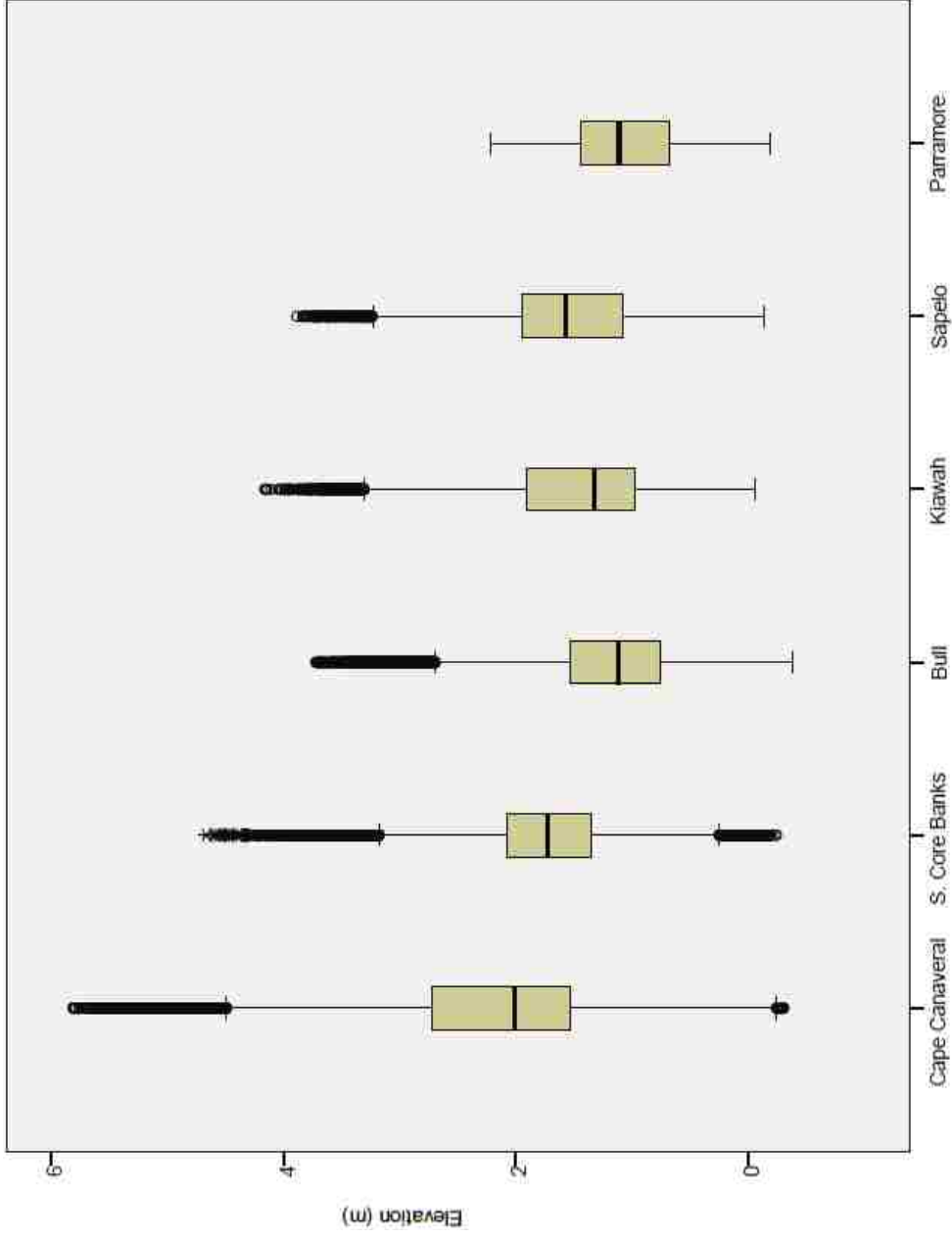




Figure 4.4e. Sapelo Island, Cluster 6, and AOIs (in red).



**Figure 4.4f.** Cape Canaveral, Cluster 7, and AOIs (in red).



**Figure 4.5.** Frequency distribution of elevations among AOIs for each island sampled. The solid black line is the 50th percentile (median) elevation. The top and bottom of the box plot indicate the 75th and 25th percentile respectively. Points outside of the whiskers indicate outlier elevations

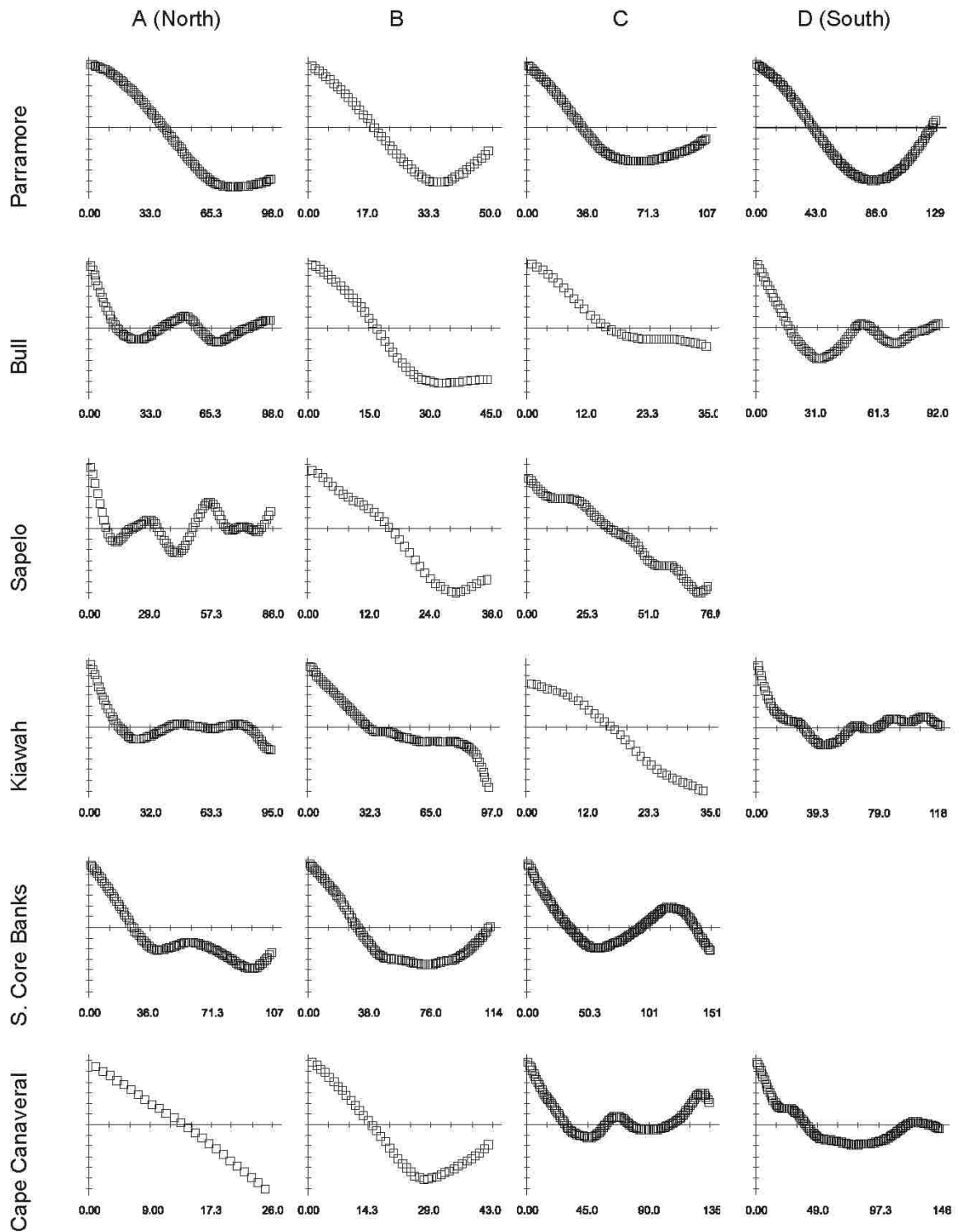


**Figure 4.6.** Correlograms produced for AOIs A (northernmost) thru B (southernmost) on each representative island. Distance classes (in meters) are plotted on the x-axis and Moran's I values, which range from 0 (negative autocorrelation) to 1 (positive autocorrelation), are plotted on the y-axis.

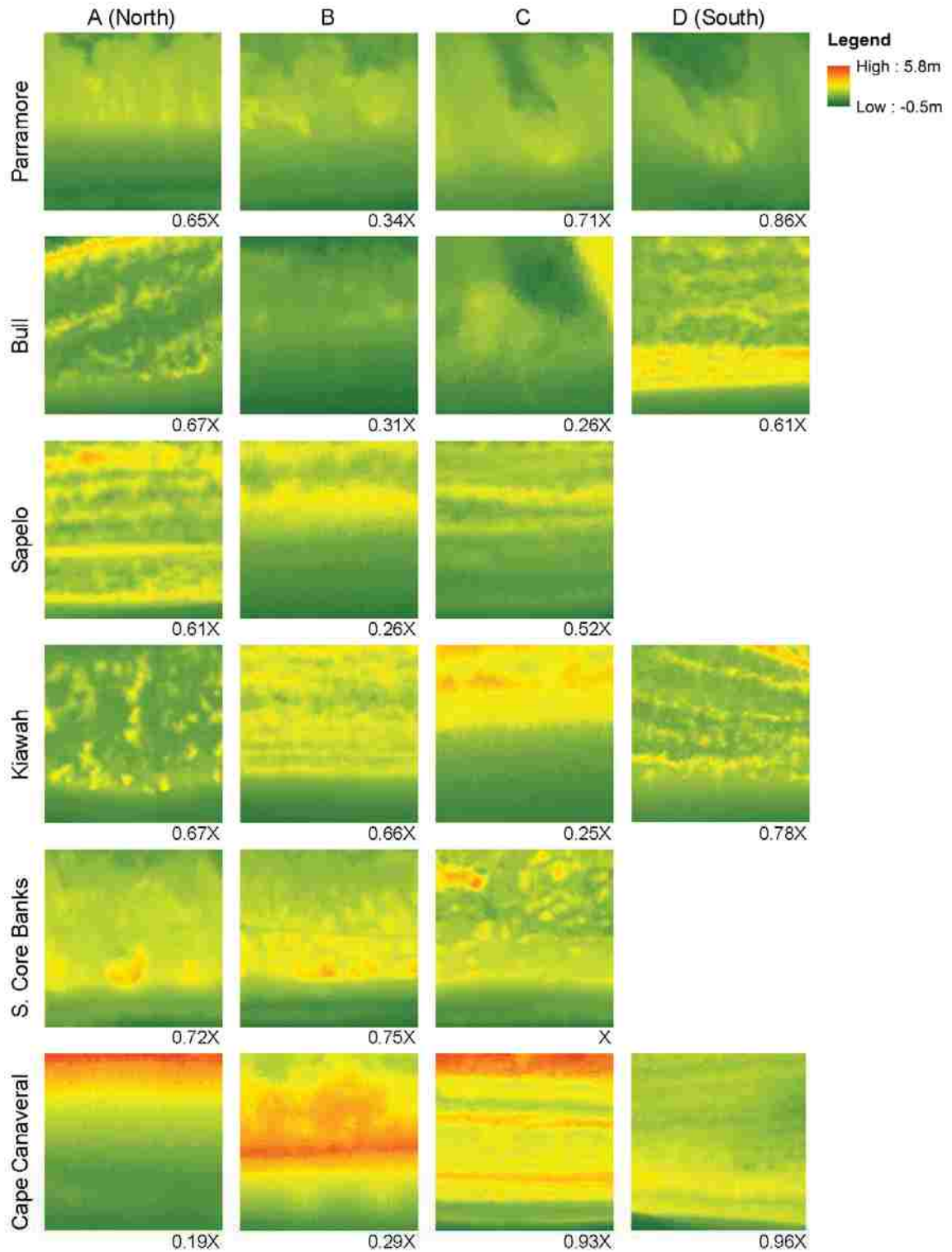


**Figure 4.7.** Reclassified AOIs A (northernmost) thru B (southernmost) used for deriving FRAGSTATS indices. AOIs differed in their dimensions. Values on the bottom right of each AOI indicate their true size relative to the largest AOI, South Core Banks C (X = 215 m<sup>2</sup>).

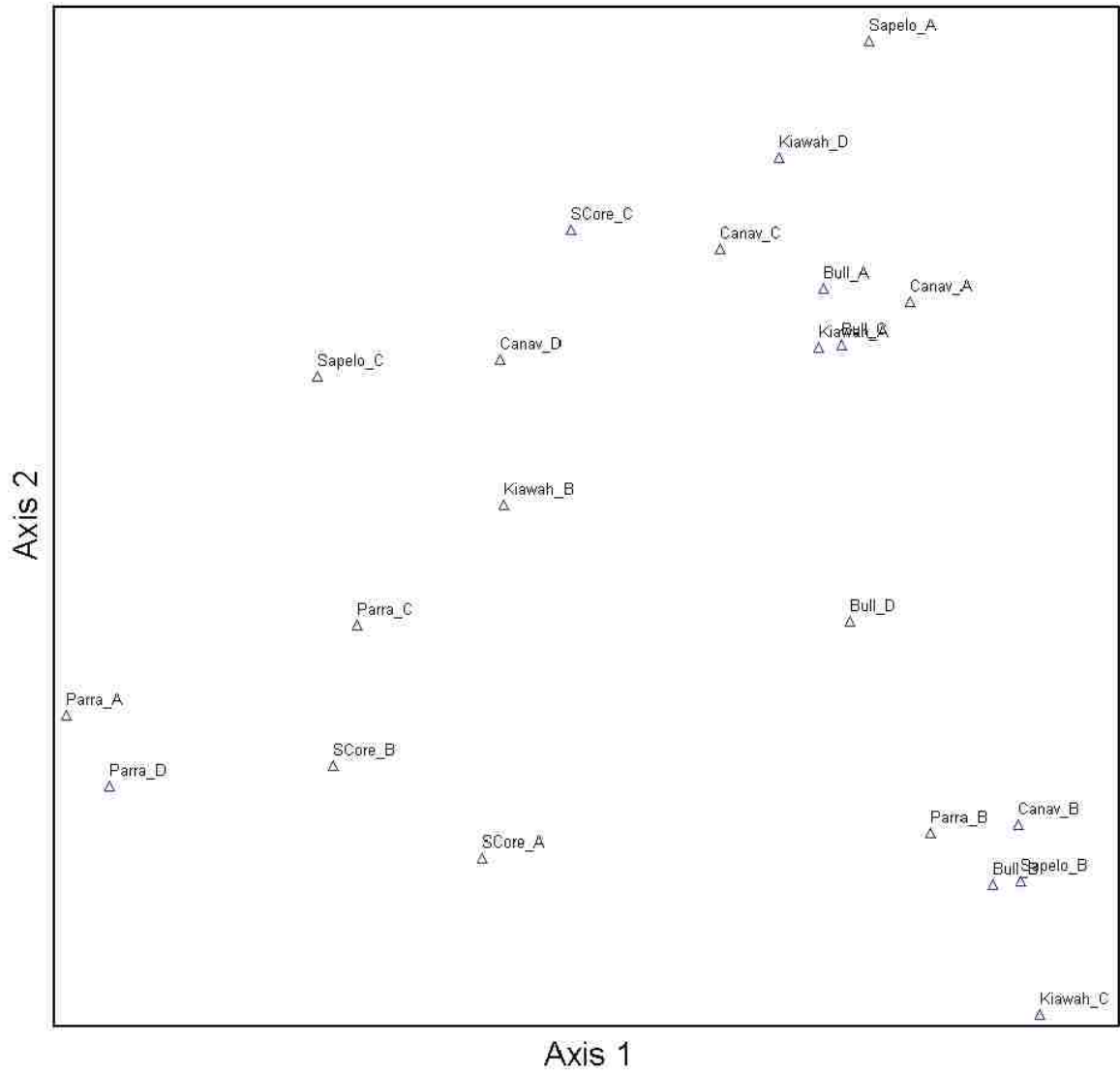


**Figure 4.8.** PCoA of spatial autocorrelation data.

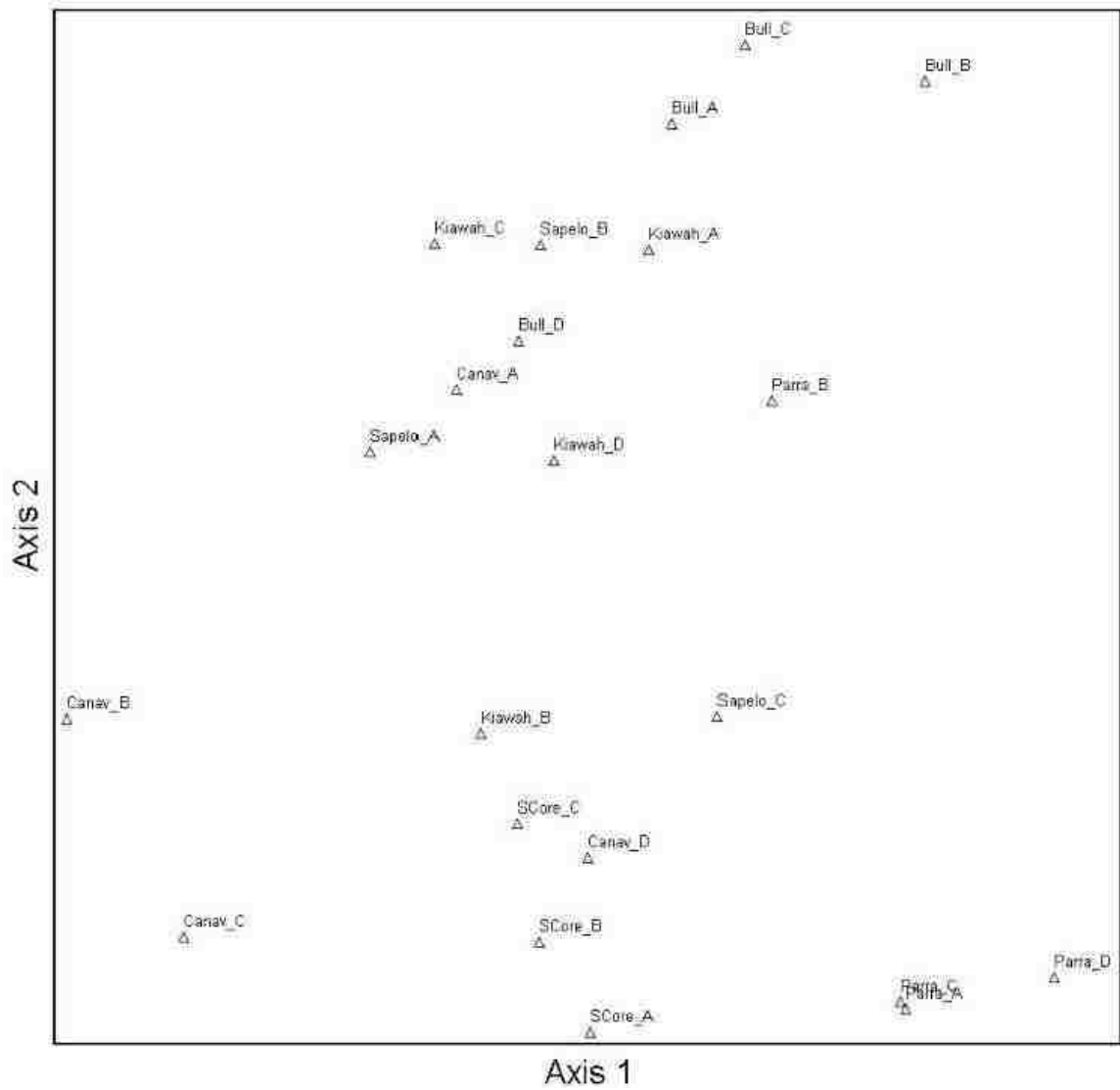


**Figure 4.9.** PCoA of dune variables AI, PAFRAC, SHAPE\_AM and Mean.

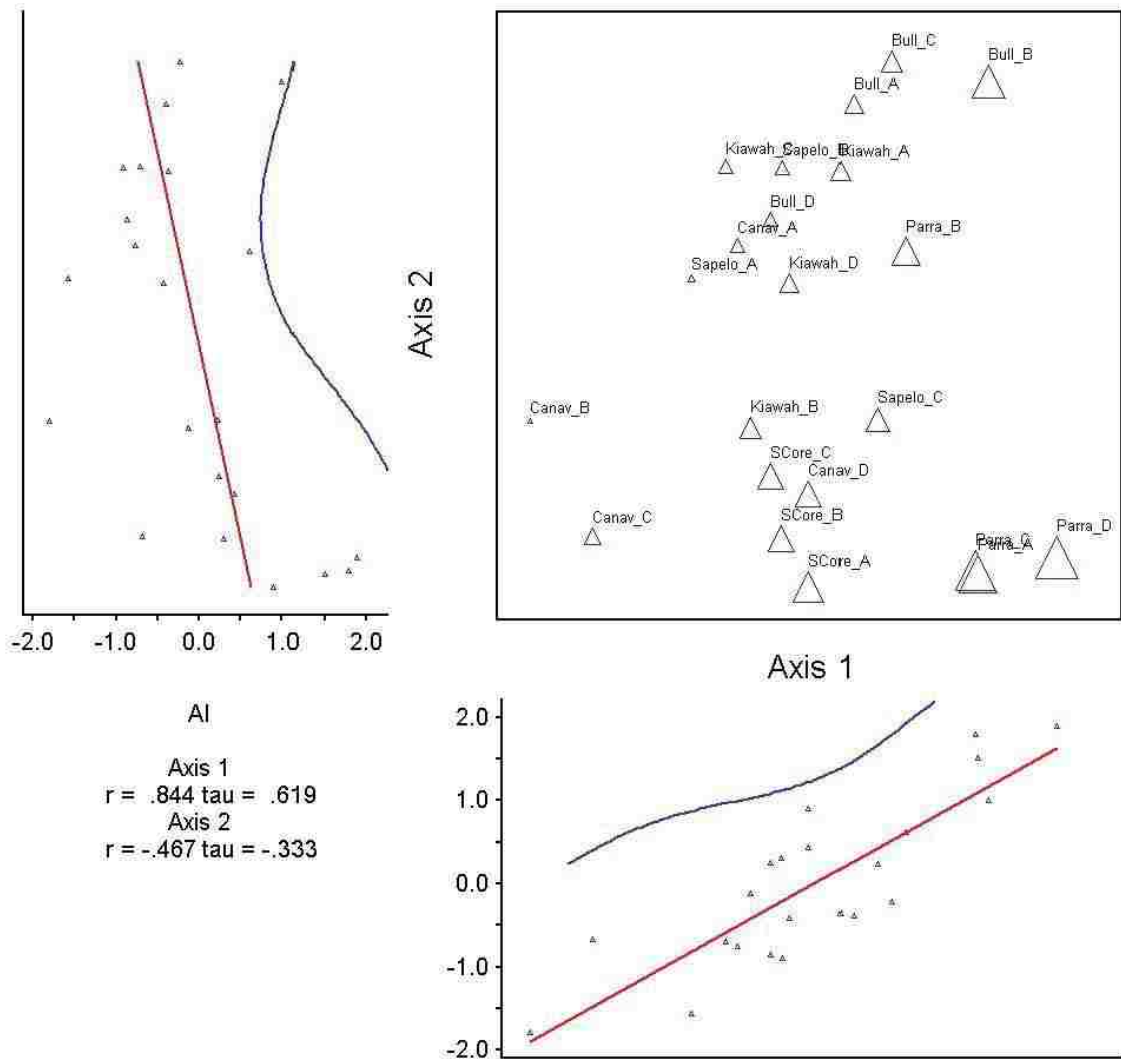


**Figure 4.10a.** PCoA plot for AI. On bottom left corner of the scatterplot are correlation coefficients  $r$  (Pearson) and  $\tau$  (Kendall) for axis scores and variables. Size of each correlation coefficient reflects the magnitude of the variable.



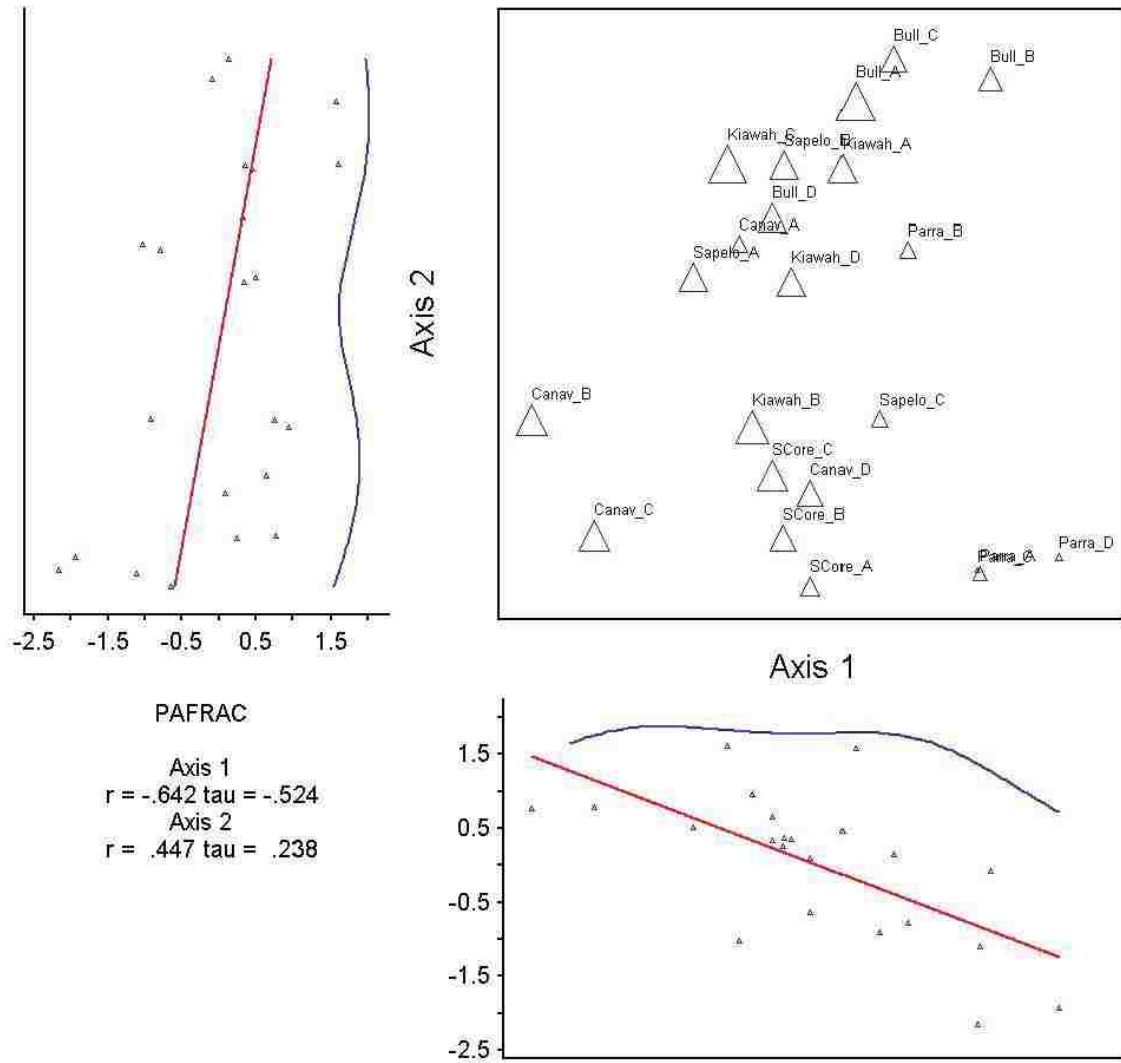


**Figure 4.10b.** PCoA plot for PAFRAC.

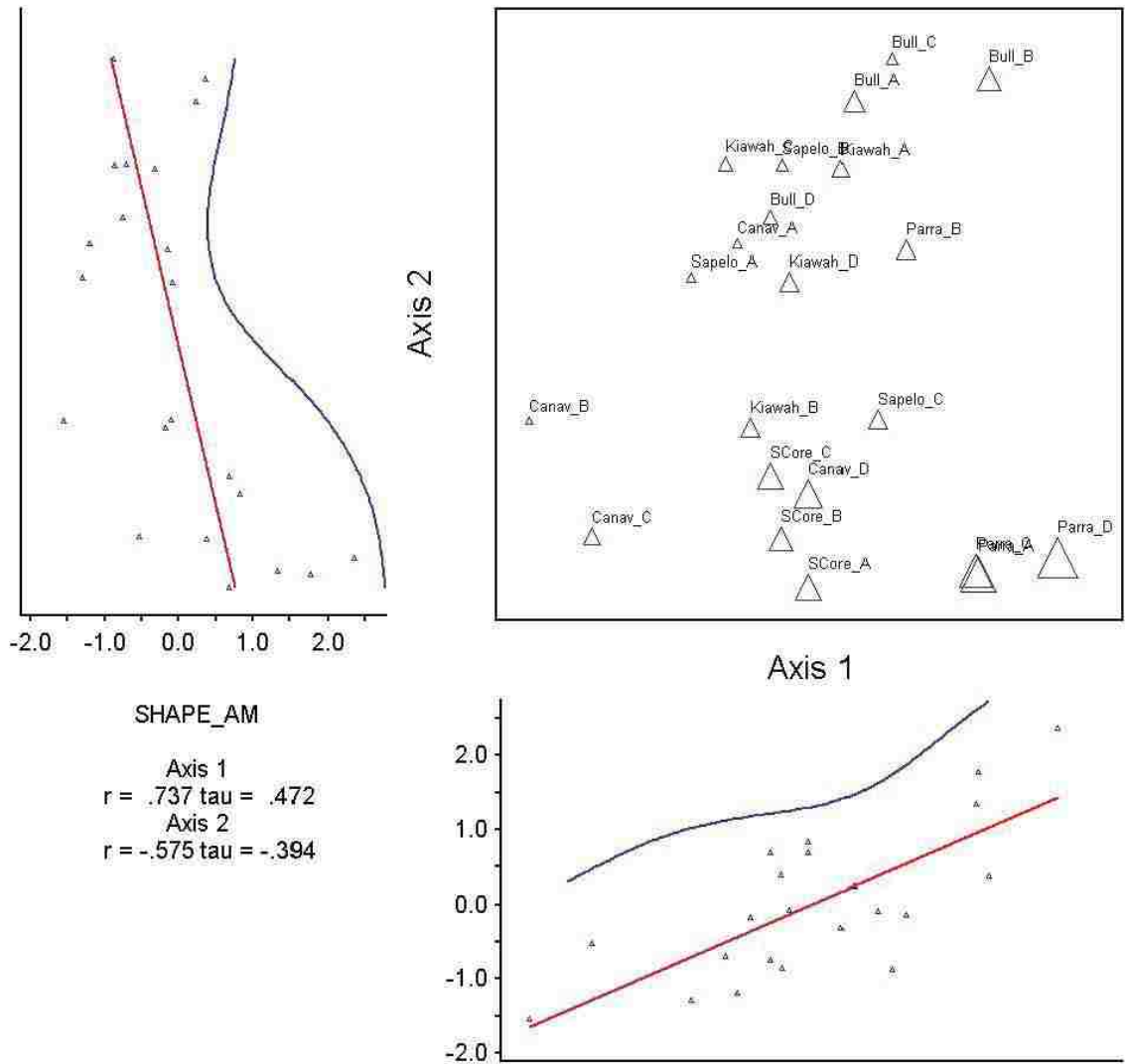


Figure 4.11a. PCoA plot for SHAPE\_AM.

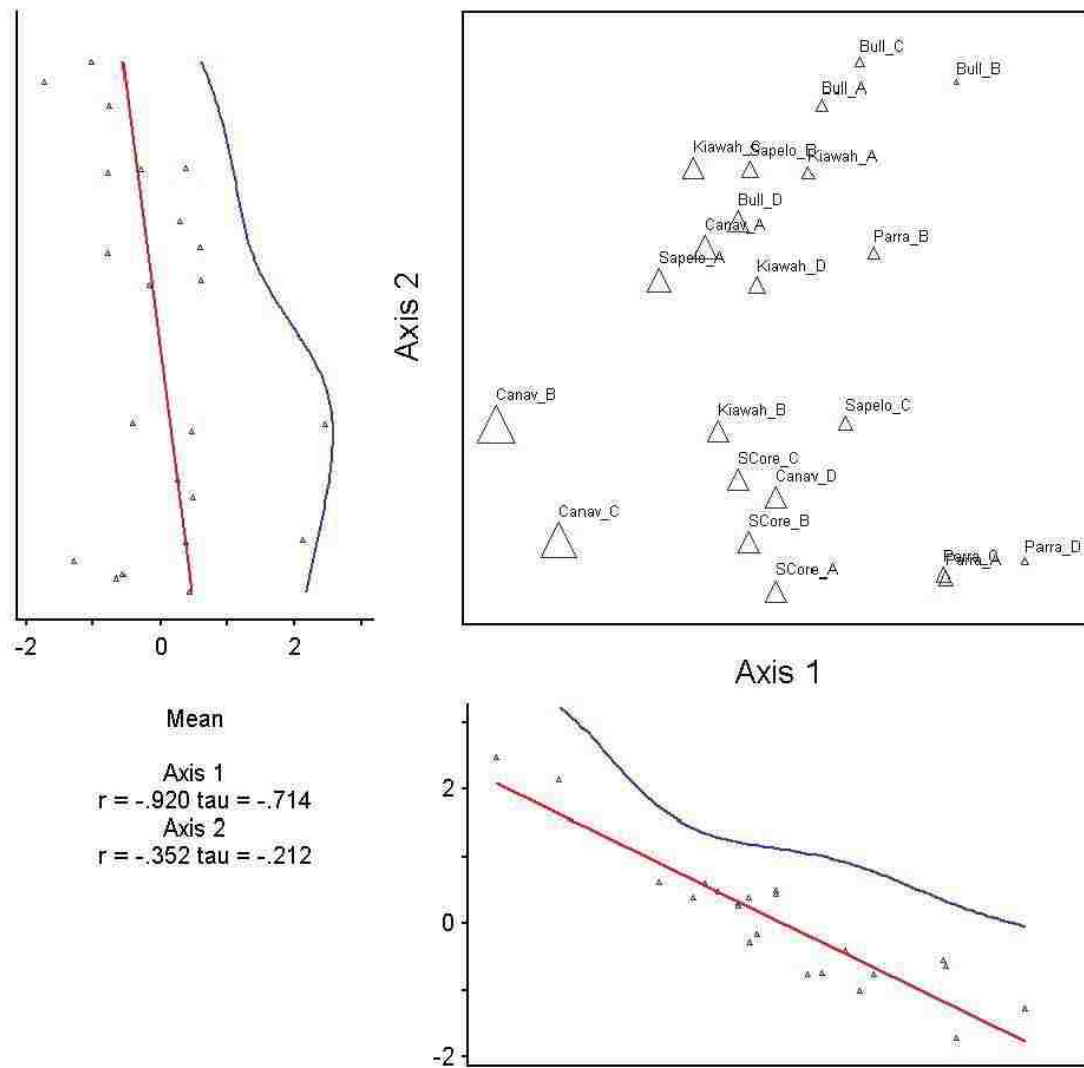


Figure 4.11b. PCoA plot for mean elevation.

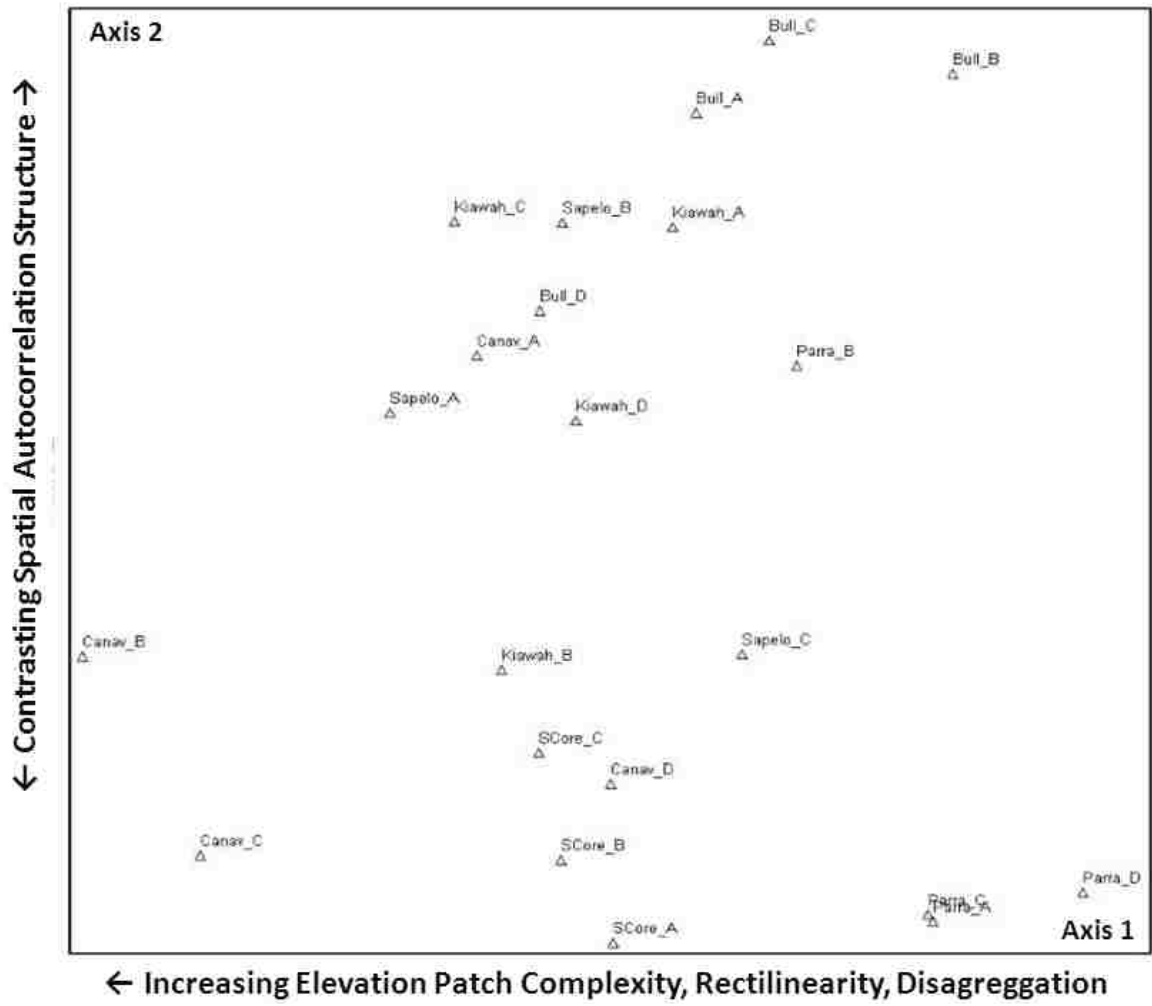


Figure 4.12. PCoA of dune topographic state space.

## CHAPTER FIVE: DISCUSSION

**Overview.** Seven morphological clusters were selected to begin the stepwise hierarchical assessment of how dune topography coincided with different clustering solutions for barrier island morphology. Williams and Leatherman (1993) identified five classes of islands, and like their study, I found evidence that broad continuum concepts of barrier island morphology were not entirely evident and that stretches of the coast are made up of multiple island morphologies. The Georgia and South Carolina Sea islands (Cluster 3 and 4) retained their prominent grouping as in the Williams and Leatherman's (1993) classification. The Florida limb of the Georgia Bight was divided up into three island morphologies, one of which is comprised of highly anthropogenic islands located in southern Florida (Cluster 1). Two of the seven morphologies identified were widely distributed (Cluster 2 and Cluster 6). Where the morphology of the mainland takes on a different form and orientation, there were often changes in the type of island morphology. This may have been related to processes of shoreline evolution (Ashton and Murray, 2006), although my classification here is more time-static in nature.

The process of classification was not without its own subjectivities. Even with the use of vector shorelines and Google Earth photos, it was difficult to identify the boundaries of some islands. This was particularly so in regions of North Carolina and South Carolina where there was a greater turnover in macroscale morphology over small distances. In part, the difficulty of isolating an island for analysis may have shaped my outcomes. On the other hand, one may consider that these stretches of coast represent locations where not a single morphologic type may be dominant and represent transitional areas.

ISA of the dune metrics indicated that the three-island grouping was optimal for discriminating among macroscale morphologic groups. Between and within group similarities in dune metrics for island sites were best developed at this hierarchical level. However, when these ten dune metrics were combined into a single data set, the resulting PCoA scatterplot suggested a single large division between the islands. These two clusters corresponded to the microtidal – mesotidal grouping that was the basis for Hayes' (1979) barrier island morphologies. The mesotidal islands, Sapelo, Bull, and Kiawah, are all found along the center of the Georgia Bight. The microtidal barrier islands, Core Banks and Cape Canaveral, are located on the limbs of the Georgia Bight.

Parramore, a rapidly retreating barrier island, was positioned near the microtidal barrier islands in the final PCoA, but its position in the scatterplot indicates that it may define its own domain. The patterns of patch-shape complexity and aggregation inferred by FRAGSTATS variables corresponded to this microtidal-mesotidal grouping.

Although island morphology formed seven clusters, the results of this study suggest that dune topography may not exhibit the same degree of difference. Two to three domains of dune topography were evident based on the derivation of a set of discriminatory variables, with some evidence suggesting that a few island sites have jumped domains. Dune topography, given its controls acting over small temporal and spatial scales, may converge to a couple of basic forms. The two to three dune topographies exhibited among islands consisted of a microtidal dune topography and a mesotidal dune topography. Their separation in their PCoA state space suggests a propensity for thresholds. Coastal landforms have thresholds or tipping points of geomorphic stability and when these limits are exceeded on barrier islands the following behaviors could unfold: increased rate of landward migration of the barrier, decreased barrier width and elevation of barrier and sand dunes, increased frequency of storm overwash, increased frequency of barrier breaching and inlet formation and widening, and segmentation of the barrier (Williams, 2013; Gutierrez et al., 2007).

Tentatively, an island site located in the empty central region of the scatterplot would exist at an intermediate level of these landscape pattern-process relationships. Some of those sites that are near this fold in the middle of the scatterplot, particularly Parramore B, Sapelo C, and Kiawah B, may have jumped from one landscape pattern-process relationship to another. Inspection of air photos and the dune metrics for Parramore B, Kiawah B, and Sapelo C suggest that they differ from the other sites on the same island. Sapelo C is located at the southernmost end of the island, which is a low lying area subject to overwash. In contrast, Sapelo A and Sapelo B have well-developed dune ridges. Kiawah B is in an area that has human development and may have undergone dune management practices. Parramore B is a site on an actively overwashed island where woody vegetation extends close to the shore. Aerial photography suggests that overwash has not been active in this area as it has been in other locations on Parramore. This is either because it is scarped or the forest vegetation alters the development of overwash topographies.

To an extent, my findings are constrained by the temporal resolution of LIDAR data, as they are often collected for generating post-storm assessments. In this study, I was relegated to using post-storm data for two of the six islands (Parramore Island and South Core Banks), due to the unavailability of processed data sets from the most recently available pre-storm years. Yet to counter this bias, one can reason that the use of different data sets for these islands capture the range of possible conditions, and that my sampling does capture a propensity for certain forms to be expressed within certain areas even with the passage of a recent hurricane. In other words, hurricanes and extratropical storms contribute to part of the morphology that is expressed and is not entirely a bias. In fact, one could reason that leaving out post-storm events may bias the description of the dunes to a form that leaves out topographies that do get expressed. Another constraint is that only dune topographies from six islands were compared and more islands would need to be sampled to get a much broader picture of dune topography. However, LIDAR data may not be fully available or of more limited quality to accomplish this. Development of spatially referenced ground-based or remote unmanned aerial vehicle photography and structure from motion photography would be one way to circumvent the dependency on LIDAR. Lastly, my findings could be strengthened by the inclusion of topographies on islands with significant human impacts (Jackson and Nordstrom, 2011; Grafals-Soto, 2012). As these islands and dunes from outlier islands are assessed, the parameters of dune state space can be more precisely defined.

## CHAPTER SIX: CONCLUSIONS

Coastal dune studies often focus on single island descriptions, capturing the uniqueness that does typify any island. On the other hand, there are commonalities among islands that merit description. This research attempted to bridge this scalar and methodological divide. I accomplished this by first dismantling the idea of a smooth continuum of barrier island morphologies. Considerable heterogeneity exists in barrier island morphologies, and along some stretches of the coast, these morphologies become geometrically complex to the extent that island classifications may be too rigid of a way to conceptualize the coast. I next documented the similarities and differences in dune topography within and between these island morphologies. To do this, a combination of spatially explicit and non-spatial metrics were obtained, including elevational frequency distributions, spatial autocorrelation of elevation at different distance classes, and FRAGSTATS indices of landscape structure. Comparisons of dune topographies using the most discriminatory dune metrics revealed two major domains of barrier island dune topography. The broad continuum classification of mesotidal and microtidal barrier island morphologies reappeared as two domains in the dune topographic state space. In addition to this was a third, smaller domain characterized by low elevations, simple patch structure, and frequent overwash as exemplified on Parramore Island. While my results dissected the idea of a smooth geographic continuum in basic barrier island morphologies, the topographies they are associated with reappeared in the spatial topology of island sites based on their dune topographies. There was morphological evidence that some island sites can jump from one domain to another. Human impacts and changes in the frequency of overwash from the natural background level may create a topography that resembles one from another domain. In other words, some within-island topographies can be more similar to islands outside of the macroscale morphology they fall within.

Speculatively, it might be reasonable to assume, as a kind of null hypothesis, that any island might contain all possible dune topographies (e.g. dune ridges) at some scalar extent and resolution. Some would be small and confined to a specific area: the closer one looks the more likely they can find, even with islands such as Sapelo or Kiawah, an overwashed area and a dune topography that looks like South Core Banks. Any island can potentially express a much wider range of topographies than what is immediately



evident. Integrating this kind of topological approach into coastal studies might circumvent the propensity to work with dunes in a strictly geographic sense that tends to force the idea that all islands are unique as a frame of reference. Topological approaches would also circumvent some enticements to rely upon ecological or individualistic fallacies of spatial reasoning.

Hopefully, the results of this study can be tested through the lens of dune plant biogeography, which can contribute to dune topographic surface morphodynamics (Godfrey 1977; Stallins and Parker, 2003). The major dune plants of the U.S. Atlantic coast are widely distributed and assessing their distribution within and between multiple islands may help to corroborate the results from this study. Where dune topographies correspond, as represented in my three final groups of dune topographies, there may be a propensity for entrainment of biogeomorphic processes in the island context (Stallins, 2005). If the hypothesis that plant species on barrier islands can manage gradual physical changes in the sedimentary environment up to some threshold force is correct, then ecosystem management should emphasize landscape-scale sedimentary modification rather than short-term, structural prevention of erosion at a specific location (Feagin et al., 2010).

In sum, this study developed new methods to characterize and compare dune topographies. Tracking dune topographies in a topological sense, in their similarity to other sites within and between islands may reveal more detail about future responses to higher sea levels than a singular focus on island morphology or on dune topography alone. Dune features have already begun to absorb the effects of higher water levels by moving further inland (Psuty and Silveira, 2010), however these effects may be variable along the coast since sea level is not rising in uniform manner (Nicholls and Cazenave, 2010). A strategically placed biogeomorphical tracking and surveillance of sandy barrier coastlines based on the results of this study might be one way to visualize this kind of complexity.

In the end, how you link dunes and their island morphology is a matter of purpose (Vale, 1988). For some purposes, they may be treated as the same everywhere, for other purposes they might each need to be considered uniquely. This study has taken a

middle ground approach that relied on an integration of large scale coastal classification with local dune topography.

## APPENDIX

### Appendix A. Islands studied and the variables used to classify their macroscale morphology.

|                     | Length<br>(Km) | Width<br>(Km) | Hurricane<br>Strikes<br>(1851-2012) | Tidal<br>Range<br>(m) | Wave<br>Height<br>(m) | LW<br>Ratio | Orientation<br>(Degrees) |
|---------------------|----------------|---------------|-------------------------------------|-----------------------|-----------------------|-------------|--------------------------|
| Amelia Island       | 20.9           | 2.59          | 6                                   | 1.71                  | 1.10                  | 8.1         | 112                      |
| Anastasia Island    | 23.0           | 1.43          | 9                                   | 1.31                  | 1.20                  | 16.1        | 127                      |
| Assateague Island   | 58.0           | 0.55          | 8                                   | 0.77                  | 1.23                  | 105.0       | 93                       |
| Assawoman Island    | 15.9           | 0.44          | 1                                   | 0.49                  | 1.20                  | 36.1        | 81                       |
| Bald Head Island    | 5.4            | 0.98          | 6                                   | 1.32                  | 1.20                  | 5.5         | 97                       |
| Bear Island         | 4.2            | 0.63          | 4                                   | 1.23                  | 1.10                  | 6.8         | 53                       |
| Bird Island         | 6.3            | 0.34          | 2                                   | 1.42                  | 1.00                  | 18.6        | 53                       |
| Blackbeard Island   | 9.6            | 1.11          | 4                                   | 2.09                  | 1.00                  | 8.7         | 83                       |
| Bogue Banks         | 38.9           | 0.62          | 16                                  | 0.93                  | 1.20                  | 62.6        | 34                       |
| Browns Island       | 5.2            | 0.28          | 3                                   | 1.23                  | 1.10                  | 18.6        | 56                       |
| Bull Island         | 9.4            | 1.34          | 1                                   | 1.51                  | 1.00                  | 7.0         | 67                       |
| Cape Canaveral      | 80.1           | 1.13          | 22                                  | 0.78                  | 1.25                  | 71.1        | 145                      |
| Cape Island         | 9.2            | 0.19          | 3                                   | 1.39                  | 1.02                  | 47.6        | 95                       |
| Capers Island       | 5.1            | 0.49          | 2                                   | 1.49                  | 1.00                  | 10.6        | 64                       |
| Cedar Island(a)     | 2.5            | 0.09          | 1                                   | 1.28                  | 1.10                  | 28.0        | 77                       |
| Cedar Island(b)     | 9.1            | 0.17          | 2                                   | 1.26                  | 1.10                  | 55.0        | 103                      |
| Cobb Island         | 8.1            | 0.25          | 1                                   | 1.24                  | 1.20                  | 32.8        | 82                       |
| Collins Island      | 12.5           | 0.49          | 6                                   | 1.29                  | 1.00                  | 25.5        | 106                      |
| Cumberland Island   | 27.0           | 2.21          | 6                                   | 1.95                  | 1.08                  | 12.2        | 104                      |
| Currituck Banks     | 111.7          | 0.90          | 43                                  | 0.81                  | 1.20                  | 123.5       | 134                      |
| Debidue Island      | 7.5            | 0.37          | 2                                   | 1.22                  | 1.00                  | 20.3        | 92                       |
| Edings Island       | 7.1            | 0.30          | 1                                   | 1.76                  | 1.07                  | 23.7        | 64                       |
| Figure Eight Island | 7.0            | 0.18          | 0                                   | 1.25                  | 1.00                  | 38.9        | 74                       |
| Folly Island        | 9.6            | 0.41          | 1                                   | 1.61                  | 1.00                  | 23.3        | 59                       |
| Fripp Island        | 4.9            | 0.74          | 3                                   | 1.88                  | 1.10                  | 6.6         | 55                       |
| Harbor Island       | 7.3            | 0.23          | 1                                   | 1.26                  | 1.05                  | 31.9        | 83                       |
| Hatteras Island     | 80.7           | 1.04          | 24                                  | 0.57                  | 1.49                  | 77.6        | 102                      |
| Highland Beach      | 23.3           | 0.47          | 7                                   | 0.73                  | 1.00                  | 49.8        | 107                      |
| Hillsboro Beach     | 8.6            | 0.37          | 4                                   | 0.68                  | 1.00                  | 23.3        | 110                      |
| Hilton Head Island  | 18.9           | 3.91          | 7                                   | 2.14                  | 1.40                  | 4.8         | 77                       |
| Hog Island          | 11.6           | 0.49          | 3                                   | 1.25                  | 1.10                  | 23.5        | 87                       |
| Holden Beach        | 12.9           | 0.39          | 4                                   | 1.38                  | 1.00                  | 32.8        | 32                       |
| Hutchinson Island   | 36.0           | 0.62          | 11                                  | 0.51                  | 1.22                  | 57.9        | 136                      |
| Isle of Palms Beach | 9.8            | 0.80          | 2                                   | 1.52                  | 1.00                  | 12.2        | 55                       |
| Jacksonville Beach  | 54.6           | 2.50          | 13                                  | 1.38                  | 1.10                  | 21.8        | 125                      |
| Jekyll Island       | 12.3           | 1.27          | 3                                   | 2.07                  | 1.00                  | 9.6         | 107                      |
| Jupiter Island      | 25.7           | 0.41          | 11                                  | 0.46                  | 1.10                  | 62.7        | 133                      |
| Key Biscayne        | 7.0            | 1.24          | 2                                   | 0.61                  | 0.90                  | 5.7         | 111                      |

## Appendix A (continued)

|                         |      |      |    |      |      |       |     |
|-------------------------|------|------|----|------|------|-------|-----|
| Kiawah Island           | 15.1 | 0.83 | 4  | 1.67 | 1.00 | 18.2  | 52  |
| Lauderdale-by-the-Sea   | 18.3 | 0.59 | 2  | 0.77 | 1.00 | 31.1  | 107 |
| Lighthouse Island       | 3.5  | 0.08 | 0  | 1.51 | 1.00 | 43.9  | 28  |
| Little Talbot Island    | 6.8  | 0.85 | 5  | 1.62 | 1.10 | 7.9   | 120 |
| Little Tybee Island     | 7.5  | 0.35 | 3  | 2.10 | 1.10 | 21.1  | 70  |
| Masonboro Island        | 12.3 | 0.18 | 4  | 1.23 | 1.10 | 70.5  | 93  |
| Metompkin Island        | 10.0 | 0.20 | 1  | 0.88 | 1.15 | 49.8  | 91  |
| Miami Beach             | 14.9 | 1.16 | 4  | 0.77 | 0.90 | 12.9  | 113 |
| Murphy Island           | 8.0  | 0.12 | 1  | 1.28 | 1.10 | 68.0  | 62  |
| Myrtle Island           | 2.1  | 0.07 | 1  | 1.39 | 1.10 | 29.6  | 86  |
| N. and S. Core Banks    | 39.0 | 0.26 | 13 | 0.93 | 1.29 | 152.9 | 66  |
| North Hutchinson Island | 45.5 | 0.87 | 8  | 0.71 | 1.24 | 52.1  | 134 |
| Oak Island              | 20.4 | 1.03 | 7  | 1.30 | 1.20 | 19.8  | 18  |
| Ocean Isle Beach        | 8.9  | 0.62 | 1  | 1.42 | 1.00 | 14.4  | 45  |
| Ocracoke Island         | 24.2 | 0.39 | 5  | 0.93 | 1.20 | 61.5  | 62  |
| Onslow Beach            | 11.4 | 0.16 | 2  | 1.23 | 1.10 | 70.9  | 63  |
| Ormond-by-the-Sea       | 75.4 | 0.79 | 19 | 0.88 | 1.20 | 95.6  | 146 |
| Ossabaw Island          | 14.7 | 0.39 | 4  | 2.15 | 1.00 | 37.3  | 79  |
| Palm Beach              | 25.0 | 0.33 | 7  | 0.81 | 1.00 | 76.0  | 113 |
| Parramore Island        | 9.7  | 0.45 | 1  | 1.26 | 1.10 | 21.5  | 87  |
| Pawleys Island          | 5.8  | 0.10 | 0  | 1.06 | 1.00 | 57.7  | 90  |
| Pleasure Island         | 13.7 | 1.47 | 2  | 1.20 | 1.10 | 9.4   | 97  |
| Portsmouth Island       | 30.1 | 0.33 | 4  | 0.93 | 1.27 | 91.3  | 74  |
| Saint Catherines Island | 15.8 | 1.10 | 6  | 2.15 | 1.00 | 14.4  | 102 |
| Sand Island             | 9.1  | 0.18 | 1  | 1.24 | 1.00 | 51.8  | 83  |
| Sapelo Island           | 8.1  | 0.32 | 2  | 2.09 | 1.00 | 25.1  | 83  |
| Sea Island              | 8.1  | 0.30 | 6  | 2.02 | 1.00 | 27.1  | 82  |
| Sebastian               | 62.4 | 1.15 | 14 | 0.88 | 1.25 | 54.2  | 106 |
| Shackleford Banks       | 13.8 | 0.45 | 6  | 0.93 | 1.10 | 30.9  | 0   |
| Ship Shoal Island       | 2.7  | 0.20 | 1  | 1.24 | 1.10 | 13.5  | 104 |
| Singer Island           | 19.3 | 1.36 | 5  | 0.84 | 1.03 | 14.1  | 127 |
| Smith Island            | 11.2 | 0.24 | 4  | 1.07 | 1.10 | 46.1  | 74  |
| Sullivans Island        | 4.4  | 0.64 | 2  | 1.56 | 1.00 | 6.9   | 55  |
| Sunny Isle Beach        | 21.3 | 0.41 | 9  | 0.70 | 0.90 | 52.0  | 112 |
| Topsail Island          | 35.4 | 0.27 | 6  | 1.23 | 1.00 | 131.1 | 65  |
| Tybee Island            | 4.7  | 1.44 | 4  | 2.10 | 1.10 | 3.3   | 113 |
| Wassaw Island           | 8.3  | 0.79 | 4  | 2.15 | 1.10 | 10.5  | 74  |
| Waties Island           | 4.3  | 0.65 | 3  | 1.44 | 1.00 | 6.7   | 37  |
| Wreck Island            | 4.1  | 0.19 | 4  | 1.24 | 1.10 | 21.9  | 119 |

**Appendix B.** Descriptive variables derived from elevation data corresponding to each AOI.

| Island         |   | Mean | Minimum | Maximum | Skewness | Kurtosis | 25 <sup>th</sup> % | Mode | 75 <sup>th</sup> % |
|----------------|---|------|---------|---------|----------|----------|--------------------|------|--------------------|
| Parramore      | A | 1.11 | -0.07   | 2.21    | -0.37    | -1.33    | 0.51               | 1.32 | 1.67               |
|                | B | 1.04 | -0.19   | 2.15    | -0.26    | -0.64    | 0.68               | 1.07 | 1.44               |
|                | C | 1.16 | -0.19   | 2.10    | -0.58    | -0.34    | 0.87               | 1.25 | 1.46               |
|                | D | 0.77 | -0.28   | 1.87    | -0.14    | -0.97    | 0.42               | 0.84 | 1.10               |
| Bull           | A | 1.06 | -0.31   | 3.69    | 1.50     | 3.23     | 0.72               | 0.92 | 1.26               |
|                | B | 0.53 | -0.38   | 1.51    | -0.34    | -1.05    | 0.19               | 0.63 | 0.89               |
|                | C | 0.91 | -0.09   | 2.78    | 1.03     | 0.92     | 0.40               | 0.88 | 1.16               |
|                | D | 1.62 | 0.10    | 3.72    | 0.46     | -0.20    | 1.20               | 1.44 | 2.01               |
| Sapelo         | A | 1.79 | 0.03    | 3.89    | 0.01     | 0.60     | 1.42               | 1.75 | 2.14               |
|                | B | 1.31 | -0.11   | 3.06    | 0.04     | -1.32    | 0.52               | 1.38 | 2.04               |
|                | C | 1.23 | -0.14   | 2.66    | 0.05     | -0.74    | 0.73               | 1.20 | 1.67               |
| Kiawah         | A | 1.05 | -0.04   | 3.42    | 0.96     | 1.71     | 0.78               | 0.96 | 1.26               |
|                | B | 1.71 | -0.06   | 3.32    | -0.96    | -0.28    | 1.36               | 1.98 | 2.23               |
|                | C | 1.66 | 0.10    | 3.86    | 0.10     | -1.52    | 0.61               | 1.46 | 2.65               |
|                | D | 1.37 | 0.15    | 4.16    | 0.87     | 2.53     | 1.12               | 1.31 | 1.61               |
| S. Core Banks  | A | 1.69 | -0.24   | 3.72    | -0.14    | 0.51     | 1.26               | 1.83 | 2.03               |
|                | B | 1.67 | -0.18   | 4.02    | -0.29    | -0.39    | 1.28               | 1.69 | 2.23               |
|                | C | 1.59 | -0.18   | 4.68    | 0.06     | 0.96     | 1.25               | 1.64 | 1.99               |
| Cape Canaveral | A | 1.78 | 0.15    | 5.51    | 0.95     | -0.21    | 0.66               | 1.30 | 2.57               |
|                | B | 2.78 | 0.16    | 5.15    | -0.27    | -0.82    | 1.92               | 2.87 | 3.72               |
|                | C | 2.60 | -0.31   | 5.81    | 0.14     | 0.49     | 2.19               | 2.53 | 3.07               |
|                | D | 1.72 | -0.52   | 2.96    | -0.98    | 2.57     | 1.49               | 1.72 | 2.04               |

**Appendix C.** FRAGSTATS variables derived from reclassified rasters for each AOI.

| Island         |   | AI   | CONTAG | IJI  | LPI  | LSI  | PAFRAC | SHAPE_AM | SIDI  |
|----------------|---|------|--------|------|------|------|--------|----------|-------|
| Parramore      | A | 73.7 | 40.5   | 56.5 | 6.93 | 20.4 | 1.53   | 4.97     | 0.941 |
|                | B | 63.1 | 35.7   | 60.2 | 5.18 | 15.2 | 1.54   | 2.97     | 0.943 |
|                | C | 77.1 | 44.8   | 53.7 | 7.30 | 19.5 | 1.51   | 4.52     | 0.917 |
|                | D | 78.3 | 42.8   | 54.9 | 9.79 | 21.9 | 1.52   | 5.60     | 0.928 |
| Bull           | A | 51.3 | 41.4   | 57.2 | 7.38 | 35.4 | 1.58   | 3.37     | 0.927 |
|                | B | 67.6 | 38.3   | 57.9 | 14.0 | 11.6 | 1.55   | 3.50     | 0.909 |
|                | C | 53.2 | 35.8   | 61.8 | 5.21 | 13.2 | 1.55   | 2.20     | 0.939 |
|                | D | 45.6 | 35.1   | 62.4 | 3.54 | 37.2 | 1.56   | 2.34     | 0.944 |
| Sapelo         | A | 37.1 | 33.4   | 62.8 | 0.85 | 39.7 | 1.56   | 1.78     | 0.947 |
|                | B | 45.0 | 30.6   | 66.3 | 5.96 | 15.6 | 1.56   | 2.22     | 0.962 |
|                | C | 58.6 | 36.6   | 61.4 | 10.3 | 24.2 | 1.53   | 3.03     | 0.944 |
| Kiawah         | A | 51.5 | 41.0   | 57.5 | 4.07 | 34.4 | 1.56   | 2.78     | 0.920 |
|                | B | 54.4 | 39.6   | 54.2 | 4.12 | 33.2 | 1.56   | 2.93     | 0.940 |
|                | C | 47.5 | 34.4   | 63.6 | 7.95 | 14.8 | 1.57   | 2.38     | 0.959 |
|                | D | 50.8 | 41.3   | 57.2 | 2.91 | 42.9 | 1.56   | 3.03     | 0.928 |
| S. Core Banks  | A | 66.5 | 44.6   | 54.4 | 5.65 | 27.7 | 1.54   | 3.84     | 0.937 |
|                | B | 59.4 | 40.2   | 56.2 | 5.45 | 34.8 | 1.56   | 3.52     | 0.959 |
|                | C | 58.8 | 43.9   | 53.0 | 5.29 | 46.1 | 1.56   | 3.84     | 0.948 |
| Cape Canaveral | A | 46.7 | 37.8   | 62.7 | 13.4 | 11.9 | 1.53   | 1.87     | 0.958 |
|                | B | 34.5 | 29.6   | 66.8 | 1.27 | 22.0 | 1.56   | 1.51     | 0.975 |
|                | C | 47.8 | 39.2   | 57.8 | 3.06 | 52.1 | 1.56   | 2.57     | 0.959 |
|                | D | 61.0 | 42.1   | 53.5 | 2.58 | 42.2 | 1.55   | 3.99     | 0.929 |

## REFERENCES

- Anthony EJ. (2013) Storms, shoreface morphodynamics, sand supply, and the accretion and erosion of coastal dune barriers in the southern North Sea. *Geomorphology* 199: 8-21.
- Anthony EJ and Orford JD. (2002) Between wave- and tide-dominated coasts: The middle ground revisited. *Journal of Coastal Research* 36: 8-15.
- Arkema KK, Guannel G, Verutes G, et al. (2013) Coastal habitats shield people and property from sea-level rise and storms. *Nature Climate Change* 3: 913-918.
- Ashton AD and Murray AB. (2006) High-angle wave instability and emergent shoreline shapes: 1. Modeling of sand waves, flying spits, and capes. *Journal of Geophysical Research-Earth Surface* 111: 19.
- Bartley JD, Buddemeier RW and Bennett DA. (2001) Coastline complexity: a parameter for functional classification of coastal environments. *Journal of Sea Research* 46: 87-97.
- Burchsted D, Daniels M, Thorson R, et al. (2010) The river discontinuum: Applying beaver modifications to baseline conditions for restoration of rorested headwaters. *Bioscience* 60: 908-922.
- Cooper JAG, Pilkey OH and Lewis DA. (2007) Islands behind islands: An unappreciated coastal landform category. *Journal of Coastal Research*: 907-911.
- Coumou D and Rahmstorf S. (2012) A decade of weather extremes. *Nature Climate Change* 2: 491-496.
- Cushing CE, Cummins KW and Minshall GW. (2006) *River and Stream Ecosystems of the World*: University of California Press.
- Cushman SA, McGariyal K and Neel MC. (2008) Parsimony in landscape metrics: Strength, universality, and consistency. *Ecological Indicators* 8: 691-703.
- Davies JL. (1964) A morphogenic approach to world shorelines. *Zeitschrift für Geomorphologie* 8: 27-42.
- Davis RA. (1994) Barrier island systems: A geologic overview. In: Davis RA (ed) *Geology of Holocene Barrier Island Systems*. New York: Springer-Verlag, 1-46.
- Davis RA. (2013) A new look at barrier-inlet morphodynamics. *Journal of Coastal Research*: 1-12.
- Davis RA and Hayes MO. (1984) What is a wave-dominated coast. *Marine Geology* 60: 313-329.
- Doing H. (1985) Coastal fore-dune zonation and succession in various parts of the world. *Vegetatio* 61: 65-75.

Dufrene M and Legendre P. (1997) Species assemblages and indicator species: The need for a flexible asymmetrical approach. *Ecological Monographs* 67: 345-366.

Elko NA, Sallenger AH, Jr., Guy K, et al. (2002) *Barrier island elevations relevant to potential storm impacts; 1, Techniques*, St. Petersburg, FL: U.S. Geological Survey, Center for Coastal Geology.

Engelhart SE, Horton BP, Douglas BC, et al. (2009) Spatial variability of late Holocene and 20(th) century sea-level rise along the Atlantic coast of the United States. *Geology* 37: 1115-1118.

Evans MW, Hine AC, Belknap DF, et al. (1985) Bedrock controls on barrier-island development: West-central Florida coast. *Marine Geology* 63: 263-283.

Everard M, Jones L and Watts B. (2010) Have we neglected the societal importance of sand dunes? An ecosystem services perspective. *Aquatic Conservation: Marine and Freshwater Ecosystems* 20: 476-487.

Feagin RA, Sherman DJ and Grant WE. (2005) Coastal erosion, global sea-level rise, and the loss of sand dune plant habitats. *Frontiers in Ecology and the Environment* 3: 359-364.

Feagin RA, Smith WK, Psuty NP, et al. (2010) Barrier islands: Coupling anthropogenic stability with ecological sustainability. *Journal of Coastal Research* 26: 987-992.

Finkl CW. (2004) Coastal classification: Systematic approaches to consider in the development of a comprehensive scheme. *Journal of Coastal Research* 20: 166-213.

FitzGerald DM, Fenster MS, Argow BA, et al. (2008) Coastal impacts due to sea-level rise. *Annual Review of Earth and Planetary Sciences* 36: 601-647.

Gares PA, Wang Y and White SA. (2006) Using LIDAR to monitor a beach nourishment project at Wrightsville Beach, North Carolina, USA. *Journal of Coastal Research* 22: 1206-1219.

Godfrey PJ. (1977) Climate, plant response and development of dunes on barrier beaches along the United States East Coast. *International Journal of Biometeorology* 21: 203-215.

Gornitz V. (1991) Global coastal hazards from future sea-level rise. *Global and Planetary Change* 89: 379-398.

Gornitz VM, Daniels RC, White TW, et al. (1994) The development of a coastal risk assessment database: Vulnerability to sea-level rise in the U.S. Southeast. *Journal of Coastal Research*: 327-338.

Grafals-Soto R. (2012) Effects of sand fences on coastal dune vegetation distribution. *Geomorphology* 145: 45-55.



Grinsted A, Moore JC and Jevrejeva S. (2012) Homogeneous record of Atlantic hurricane surge threat since 1923. *Proceedings of the National Academy of Sciences of the United States of America* 109: 19601-19605.

Gutierrez BT, Williams SJ and Thieler ER. (2007) Potential for shoreline changes due to sea-level rise along the US mid-Atlantic region: U.S. Geological Survey Open-File Report 2007-1278.

Hammar-Klose ES and Thieler ER. (2001) *Coastal vulnerability to sea-level rise: A preliminary database for the U.S. Atlantic, Pacific and Gulf of Mexico coasts*. Available at: <http://pubs.usgs.gov/dds/dds68/>.

Hapke CJ, Kratzmann MG and Himmelstoss EA. (2013) Geomorphic and human influence on large-scale coastal change. *Geomorphology* 199: 160-170.

Hayden BP, Santos MCFV, Shao GF, et al. (1995) Geomorphological controls on coastal vegetation at the Virginia Coast Reserve. *Geomorphology* 13: 283-300.

Hayes MO. (1979) Barrier island morphology as a function of tidal and wave regime. In: Leatherman SP (ed) *Barrier Islands from the Gulf of St. Lawrence to the Gulf of Mexico*. New York: Academic Press, 1-27.

Hayes MO and Michel J. (2008) *A Coast for All Seasons: A Naturalist's Guide to the Coast of South Carolina*, Columbia, South Carolina: Pandion Books.

Hesp P. (2011) Dune Coasts. In: *Treatise on Estuarine and Coastal Science*. Waltham: Academic Press, 193-221.

Houser C. (2009) Synchronization of transport and supply in beach-dune interaction. *Progress in Physical Geography* 33: 733-746.

Houser C. (2013) Alongshore variation in the morphology of coastal dunes: Implications for storm response. *Geomorphology* 199: 48-61.

Houser C and Hamilton S. (2009) Sensitivity of post-hurricane beach and dune recovery to event frequency. *Earth Surface Processes and Landforms* 34: 613-628.

Houser C, Hapke C and Hamilton S. (2008) Controls on coastal dune morphology, shoreline erosion and barrier island response to extreme storms. *Geomorphology* 100: 223-240.

Isenburg M and Schewchuck J. (2007) *LAStools: converting, viewing, and compressing LIDAR data in LAS format*. Available at: <http://www.cs.unc.edu/~isenburg/lastools>.

Jackson NL and Nordstrom KF. (2011) Aeolian sediment transport and landforms in managed coastal systems: A review. *Aeolian Research* 3: 181-196.

Jackson NL, Nordstrom KF, Feagin RA, et al. (2013) Coastal geomorphology and restoration. *Geomorphology* 199: 1-7.

- Kupfer JA. (2012) Landscape ecology and biogeography: Rethinking landscape metrics in a post-FRAGSTATS landscape. *Progress in Physical Geography* 36: 400-420.
- Leatherman SP. (1978) *Barrier islands from the Gulf of St. Lawrence to the Gulf of Mexico*, New York: Academic Press.
- Legendre P. (1993) Spatial autocorrelation: Trouble or new paradigm. *Ecology* 74: 1659-1673.
- Liu H, Sherman D and Gu S. (2007) Automated extraction of shorelines from airborne light detection and ranging data and accuracy assessment based on Monte Carlo simulation. *Journal of Coastal Research*: 1359-1369.
- Magliocca NR, McNamara DE and Murray AB. (2011) Long-term, large-scale morphodynamic effects of artificial dune construction along a barrier island coastline. *Journal of Coastal Research* 27: 918-930.
- Masselink G and van Heteren S. (In press) Response of wave-dominated and mixed-energy barriers to storms. *Marine Geology*.
- Mcbride RA, Byrnes MR and Hiland MW. (1995) Geomorphic response-type model for barrier coastlines: A regional perspective. *Marine Geology* 126: 143-159.
- McCune B and Mefford MJ. (1999) *PC-ORD: Multivariate analysis of ecological data*, Glenden Beach, Oregon: MjM Software Design.
- McGarigal K, Cushman SA and Ene E. (2012) FRAGSTATS v4: Spatial Pattern Analysis Program for Categorical and Continuous Maps. University of Massachusetts, Amherst.
- McGarigal K, Tagil S and Cushman SA. (2009) Surface metrics: an alternative to patch metrics for the quantification of landscape structure. *Landscape Ecology* 24: 433-450.
- Milbert DG. (2002) *Documentation for VDatum and a datum tutorial: Vertical datum transformation software, version 1.06*. Available at: [http://vdatum.noaa.gov/download/publications/2002\\_milbert\\_VDatum106.pdf](http://vdatum.noaa.gov/download/publications/2002_milbert_VDatum106.pdf)
- Mitasova H, Hardin E, Overton MF, et al. (2010) Geospatial analysis of vulnerable beach-foredune systems from decadal time series of LIDAR data. *Journal of Coastal Conservation* 14: 161-172.
- Morton RA and Sallenger AH. (2003) Morphological impacts of extreme storms on sandy beaches and barriers. *Journal of Coastal Research* 19: 560-573.
- Murray AB, Ashton A and Arnoult O. (2001) Large-scale morphodynamic consequences of an instability in alongshore transport. *Proceedings of the Symposium on River, Coastal and Estuarine Morphodynamics, Obihiro, Japan*. 355-364.
- Nicholls RJ and Cazenave A. (2010) Sea-level rise and its impact on coastal zones. *Science* 328: 1517-1520.

- National Oceanic and Atmospheric Administration. (2014) *Historical Hurricane Tracks*. Available at: <http://www.csc.noaa.gov/digitalcoast/tools/hurricanes>.
- Oertel GF. (1985) The barrier-island system. *Marine Geology* 63: 1-18.
- Otvos EG. (2010) Definition of barrier islands: Discussion of: Pilkey, O.H.; Cooper, J.A.G., and Lewis, D.A., 2009. Global distribution and geomorphology of fetch-limited barrier islands in the *Journal of Coastal Research*, 25(4), 819–837. *Journal of Coastal Research* 264: 787-787.
- Otvos EG. (2012) Coastal barriers - Nomenclature, processes, and classification issues. *Geomorphology* 139: 39-52.
- Phillips JD. (1986) Spatial analysis of shoreline erosion, Delaware Bay, New Jersey. *Annals of the Association of American Geographers* 76: 50-62.
- Poole GC. (2002) Fluvial landscape ecology: Addressing uniqueness within the river discontinuum. *Freshwater Biology* 47: 641-660.
- Psuty NP. (1988) Sediment budget and dune/beach interaction. *Journal of Coastal Research*: 1-4.
- Psuty NP and Silveira TM. (2010) Global climate change: An opportunity for coastal dunes? *Journal of Coastal Conservation* 14: 153-160.
- Richardson TM and McBride RA. (2007) Historical shoreline changes and morphodynamics of Parramore Island, Virginia (1852–2006). *Coastal Sediments*. 3647-3377.
- Riggs SR. (2007) Effect of storms on barrier island dynamics, Core Banks, Cape Lookout National Seashore, North Carolina, 1960-2001.
- Riggs SR, Cleary WJ and Snyder SW. (1995) Influence of inherited geologic framework on barrier shoreface morphology and dynamics. *Marine Geology* 126: 213-234.
- Robertson G. (2000) *GS+: Geostatistics for the environmental sciences*. Plainwell, Michigan: Gamma Design Software.
- Schlacher TA, Schoeman DS, Dugan J, et al. (2008) Sandy beach ecosystems: Key features, sampling issues, management challenges and climate change impacts. *Marine Ecology-an Evolutionary Perspective* 29: 70-90.
- Sherman DJ and Bauer BO. (1993) Dynamics of beach-dune systems. *Progress in Physical Geography* 17: 413-447.
- Spalding MD, Mclvor AL, Beck MW, et al. (2013) Coastal ecosystems: A critical element of risk reduction. *Conservation Letters*: 1-9.
- Stallins JA. (2005) Stability domains in barrier island dune systems. *Ecological Complexity* 2: 410-430.

- Stallins JA and Parker AJ. (2003) The influence of complex systems interactions on barrier island dune vegetation pattern and process. *Annals of the Association of American Geographers* 93: 13-29.
- Stone GW, Liu BZ, Pepper DA, et al. (2004) The importance of extratropical and tropical cyclones on the short-term evolution of barrier islands along the northern Gulf of Mexico, USA. *Marine Geology* 210: 63-78.
- Strauss BH, Ziemiński R, Weiss JL, et al. (2012) Tidally adjusted estimates of topographic vulnerability to sea level rise and flooding for the contiguous United States. *Environmental Research Letters* 7: 12.
- Stutz ML and Pilkey OH. (2002) Global distribution and morphology of deltaic barrier island systems. *Journal of Coastal Research* 36: 694-707.
- Stutz ML and Pilkey OH. (2011) Open-ocean barrier islands: Global influence of climatic, oceanographic, and depositional settings. *Journal of Coastal Research* 27: 207-222.
- Su L and Gibeaut J. (2010) An improved classification approach for LIDAR point clouds on Texas coastal areas. *A special joint symposium of ISPRS Technical Commission IV & Auto-Carto in conjunction with ASPRS/CaGIS 2010 Fall Specialty Conference*. Orlando, Florida.
- Temmerman S, Meire P, Bouma TJ, et al. (2013) Ecosystem-based coastal defence in the face of global change. *Nature* 504: 79-83.
- Thorp JH, Thoms MC and Delong MD. (2010) *The Riverine Ecosystem Synthesis: Toward Conceptual Cohesiveness in River Science*: Elsevier.
- Vale TR. (1988) Clear-cut logging, vegetation dynamics, and human wisdom. *Geographical Review* 78: 375-386.
- Williams AT and Leatherman SP. (1993) Process-form relationships on USA East-Coast barrier islands. *Zeitschrift für Geomorphologie* 37: 179-197.
- Williams SJ. (2013) Sea-Level Rise Implications for Coastal Regions. *Journal of Coastal Research* 63: 184-196.
- Woodruff JD, Irish JL and Camargo SJ. (2013) Coastal flooding by tropical cyclones and sea-level rise. *Nature* 504: 44-52.
- Zhang KQ and Leatherman S. (2011) Barrier island population along the US Atlantic and Gulf Coasts. *Journal of Coastal Research* 27: 356-363.

## VITA

### **Place of birth**

Ponce, Puerto Rico

### **Academic history**

B.S. Geography, Florida State University (2012)

B.S. Biological Science, Florida State University (2012)

### **Professional positions**

Co-instructor in Geography (2014)

Teaching Assistant in Geography (2012 – 2013)

Research Assistant in Geography (2013)

Teaching Assistant in Biology (2010 – 2012)

### **Professional publication(s)**

Monge, J.A. and Gornish, E.S. (2014). Positive species interactions as drivers of vegetation change on a barrier island. *Journal of Coastal Research*. In press. DOI: <http://dx.doi.org/10.2112/JCOASTRES-D-12-00235.1>